Kaunas University of Technology

Faculty of Mathematics and Natural Sciences

Investigation of Emission Phenomena of Novel Organic Luminophores Towards Efficient Optoelectronic Devices

Master's Final Degree Project

Matas Gužauskas

Project author

Dr. Dmytro Volyniuk

Supervisor

Kaunas, 2020

Kaunas University of Technology

Faculty of Mathematics and Natural Sciences

Investigation of Emission Phenomena of Novel Organic Luminophores Towards Efficient Optoelectronic Devices

Master's Final Degree Project

Material science (6211FX009)

Matas Gužauskas

Project author

Dr. Dmytro Volyniuk

Supervisor

Assoc. prof. dr. Aleksandras Iljinas

Reviewer

Kaunas, 2020

Kaunas University of Technology

Faculty of Mathematics and Natural Sciences

Matas Gužauskas

Investigation of Emission Phenomena of Novel Organic Luminophores Towards Efficient Optoelectronic Devices

Declaration of Academic Integrity

I confirm that the final project of mine, Matas Gužauskas, on the topic „Investigation of Emission Phenomena of Novel Organic Luminophores Towards Efficient Optoelectronic Devices“ is written completely by myself; all the provided data and research results are correct and have been obtained honestly. None of the parts of this thesis have been plagiarised from any printed, Internet-based or otherwise recorded sources. All direct and indirect quotations from external resources are indicated in the list of references. No monetary funds (unless required by Law) have been paid to anyone for

any contribution to this project.

I fully and completely understand that any discovery of any manifestations/case/facts of dishonesty inevitably results in me incurring a penalty according to the procedure(s) effective at Kaunas University of Technology.

Matas Gužauskas

(name and surname filled in by hand) (signature)

Gužauskas, Matas. Investigation of Emission Phenomena of Novel Organic Luminophores Towards Efficient Optoelectronic Devices. Master's Final Degree Project supervisor dr. Dmytro Volyniuk; Faculty of Mathematics and Natural Sciences Kaunas University of Technology.

Study field and area (study field group): Technological Sciences, Materials Technologies (F03).

Keywords: organic, semiconductor, OLED, sensor.

Kaunas, 2020. Number of pages: 50 p.

Summary

Organic luminophores are widely used as active materials in various optoelectronic devices including organic light-emitting diodes (OLEDs) and optical sensors. Further generation of organic luminophores with enhanced or even unique properties can predictively leads to improvement efficiency of known optoelectronic devices or even to discovery of novel devices. Newly designed and synthesised derivatives of 5,5-dioxi-phenothiazine, benzophenone and sulfonyldi-4,1-phenylene, bis[4-(5,5-dioxo-10H-phenothiazin-10-yk)phenyl]methanone (compound 1) and 10,10'-(sulfonyldi-4,1-phenylene)bis-10H-phenothiazine-5,5-dioxide (compound 2) were selected for this study aiming to find their most appropriate applications in optoelectronic devices. With such propose, photophysical properties of compounds 1 and 2 in different media were provided using various spectroscopic techniques, such as photoluminescence spectra measurement at different temperature and time-resolved fluorescence spectroscopy. Both materials emitted blue light under UV excitation in low-polarity solutions and solid-state film. Moreover, those materials were characterised by thermally activated delayed fluorescence which allows harvesting of both singlet and triplet excitons in OLEDs under electrical excitation required for 100% of internal quantum efficiency of such devices. When compounds 1 and 2 were used as emitting layer in OLEDs, the fabricated devices showed maximum external quantum efficiency (EQE) up to 1.2%. Such relatively low EQE is related to low photoluminescent quantum yield (up to 9.3%) of the studied compounds in solid films. Fortunately, compound 1 showed external stimuli responsive fluorescence behaviour being good for optical sensors. Intensity enhancements (up to 83 times) and colour high-energy shifts (in the range of CIE coordinates from (0.29; 0.45) to (0.17; 0.16)) were detected for solutions of compounds 1 under different doses of UV excitation. Due to the best of our knowledge, such phenomenon was first time observed here for acceptor*-acceptor-acceptor*type organic luminophores. Such fluorescence behaviour of compound 1 is most probably attributed to its conformational changes under external stimuli. It was demonstrated that detected properties of compounds 1 can be useful for its unique applications in ultraviolet radiation dosimeters. Under UV power in the range of 0-350 μW, DMF solutions of compound 1 showed linear UV response with slope of 115500 (R^2=0.93) demonstrating very high UV sensitivity.

Gužauskas, Matas, Emisijos reiškinio tyrimas naujuose organiniuose liuminoforuose skirtuose efektyviems optoelektroniniams prietaisams. Magistro / Profesinių studijų baigiamasis projektas / vadovas dr. Dmytro Volyniuk; Kauno technologijos universitetas, Matematikos ir Gamtos Mokslų fakultetas.

Studijų kryptis ir sritis (studijų krypčių grupė): Technologijų mokslai, Medžiagų technologijos (F03).

Reikšminiai žodžiai: organinis, puslaidininkis, OLED, sensorius.

Kaunas, 2020. Puslapių sk. 50 p.

Santrauka

Organiniai liuminoforai plačiai naudojami įvairiuose optoelektroniniuose prietaisuose kaip organiniai šviesą skleidžiantys diodai (OLED) ir optiniuose sensoriuose. Nauji organiniai liuminoforai su geresnėmis ar net unikaliomis savybėmis gali padidinti žinomų optoelektroninių prietaisų efektyvumą ar net leisti atrasti naujas šių medžiagų pritaikymo galimybes. Sukurti nauji junginiai su 5, 5-dioksi-fenotiazino, benzonono ir sulfodnil-4,1-phenileno fragmentais, bis[4-(5,5-diokso-10H-fenotiazin-10-ik)fenil]metanonas (1) ir 10,10'-(sulfonyldi-4,1-fenilene)bis-10H-phenotiazine-5,5-dioksidas buvo tiriami šiame darbe siekiant surasti labiausiai tinkamą pritaikymą. Su šiuo tikslu, šios dvi medžiagos buvo tiriamos įvairiais spektroskopiniais metodais, tokiais kaip fotoliuminescencijos priklausomybė nuo temperatūros. Abi medžiagos, 1 ir 2, pasižymėjo mėlynos spalvos emisija, tiek kietos būsenos bandiniuose, tiek silpnai poliškuose tirpaluose. Taip pat, abiejų medžiagų emisija galima charakterizuoti kaip termiškai aktyvuota uždelsta fluorescencija, kas leistų pasiekti 100 % vidinį kvantinį efektyvumą. Dėl to, šios medžiagos buvo naudotos organiniuose šviestukuose kaip šviesą skleidžiantys sluoksniai. OLED prietaisai su 1 ir 2 medžiaga pasiekė 1,2 % išorinį kvantinį efektyvumą. Tokie sąlyginai žemi efektyvumai yra susiję dėl žemų fotoliuminescencijos kvantinių išeigų kietos būsenos bandiniuose (iki 9,3 %). Šio tyrimo metu medžiagoms 1 ir 2 buvo taikomas apdorojimas UV šviesa. Šis eksperimentas parodė, kad tirpalus su medžiaga 1 paveikus UV šviesa, tirpalo emisinės savybės pasikeičia. Taigi, šitame darbe pirma kartą aprašomas sustiprintos emisijos fenomenas, kuomet emisijos spalva pasikeičia, o intensyvumas išauga, sukeltas UV spinduliuotės. Žinant tai, fotofizikinės savybės apdorotų 1 tirpalų buvo tiriamos. Pastebėta, kad apdorojant UV šviesa intensyvumas gali išaugti net iki 83 katrų, o emisijos spektras pasislinkti iki 88 nm link didesnės energijos bangos ilgių (CIE koordinačių sistemoje spektrų padėtis pasikeičia iš (0,29; 0,45) į (0,17; 0,16)). Medžiagos 1 emisijos fenomenas paaiškintas UV spinduliuotės sukeltu molekulės konformacijos pakitimu. Buvo parodyta, kad atrastos medžiagos 1 savybės gali būti naudingos kaip unikalus UV spinduliuotės dozimetru. Medžiaga 1 DMF tirpale 0-350 μW UV galios regione parodė linijinę priklausomybę su 115500 (R^2=0.93) krypties koeficientu, kas rodo stiprų jautrumą UV spinduliuotei.

Table of contents

List of figures

List of tables

List of abbreviations and terms

Abbreviations:

MO – molecular orbital

HOMO -highest occupied molecular orbital

LUMO – lowest unoccupied molecular orbital

UV – ultraviolet

IR – infrared

PLQY – photoluminescence quantum yield

ISC – intersystem crossing

TADF – Thermally activated delayed fluorescence

CT – charge transfer

RISC – reverse intersystem crossing

D – donor

A – acceptor

OLED – organic light emitting diode

HIL – hole injection layer

HTL – hole transporting layer

HBL – hole blocking layer

EML – emitting layer

EBL – electron blocking layer

ETL – electron transporting layer

EIL – electron injection layer

PL – photoluminescence

PH – phosphorescence

EL – electroluminescence

CE – current efficiency

PE – power efficiency

IQE – internal quantum efficiency

EQE – external quantum efficiency

CIE - *Commission internationale de l'éclairage* (en. International commission of illumination)

THF – tetrahidrofura

DMF – N, N-dimethylformamide

C70 – [5,6]-Fullerene-C70

mCP – 9,9-(1,3-phenylene)bis-9H-carbazole

TSPO1 – diphenyl[4-(triphenylsilyl)phenyl]phosphine oxide

TPBi – 2,2′,2"-(1,3,5-benzinetriyl)-tris(1-phenyl-1-H-benzimidazole)

Introduction

Since the beginning of mankind, light was one of the most important thing in human life. As technology evolved, light sources also advanced. In the last hundred years light sources went from candles to light emitting diodes. It is hard to imagine life without artificial light, TVs, smartphones, cars, which in the past was based inorganic materials[1]. But nowadays more and more scientists and manufacturers try to incorporate organic materials into electronics devices[2] . Organic light emitting diodes are used in portable electronic displays and TVs, organic field effect transistors are used in car radios[3], digital camera manufacturers use organic materials in optical sensors to replace silicon-based photodetectors[4]. Organic semiconductors are used from emitting light to detecting it. As new organic materials are created constantly, the applicability of these materials also increases. Thus, the work is still not over. One of the biggest research topic of organic semiconductors is OLEDs[5]. Since the first OLED in 1987 by Tang and VanSlyke[6], researchers are aiming to make as perfect device as possible, with highest efficiencies. In the beginning, OLED devices used fluorescence emitters, which could only reach 25% IQE[7]. Later, phosphorescent emitters started being used, because of their ability to harvest triplets. Phosphorescent OLED could reach 100% IQE, but they used heavy metal atoms and have high roll-off percentage[8]. Later, Adachi *et al*. introduced new molecule design and emission mechanism, which harvest excitons from triplet and reach 100% IQE without using heavy metal atoms[9]. This mechanism is called thermally activated delayed fluorescence. But this mechanism has its flaws, there are more than few articles about efficient green emitters with TADF properties, but it is difficult to design TADF molecules that exceeds in blue light emission[10]. Another challenge in organic semiconductor research is finding new properties. To clarify, organic molecules react to changes in temperature, atmosphere, electromagnetic waves, which can affect their absorption, emission, charge transfer properties[11, 12, 13].

In this work, two 5, 5-dioxi phenothiazine, benzophenone and sulfonyldi-4,1-phenylene based molecules were investigated aiming to find their most appropriate applications in optoelectronic devices. We hoped that those materials may show good results in blue OLEDs. If not, their potential in optical sensors were demonstrated.

Aim of the work is to investigate nature of emission of novel selected organic luminophores towards efficient optoelectronic devices such as OLEDs or optical sensors.

To reach this goal, **followed tasks were identified:**

1. characterize photophysical and electrochemical properties of the selected presently synthesised benzophenone and sulfonyldi-phenylene derivatives towards their potential applications;
2. determinate nature of emission of the selected benzophenone and sulfonyldi-phenylene derivatives in different media according steady-state and time resolved measurements under different conditions;
3. towards optical sensor applications, investigation of photoluminescence properties of benzophenone and sulfonyldi-phenylene derivatives under external stimuli such as UV excitation;
4. test electroluminescent properties of the studied benzophenone and sulfonyldi-phenylene derivatives as emitters in OLEDs;

5. explore possible use of benzophenone and sulfonyldi-phenylene derivatives as active materials of ultraviolet radiation dosimeters.

1. Literature review

1.1. Electrical conductivity

By their conductivity properties, materials are categorized into three categories: conductors, semiconductors and isolators[14]. These categories are characterised by the position of valence and conduction band, and the band gap energy in between them. Conductors, usually metals, have good electrical conductivity properties because the valence band and conduction band overlaps, there is no band gap in between[15].Thus electrons can freely travel from valence band to conduction band. However, isolators are the opposite of conductors. Their conductive band and valence band are separated by a wide band gap, over 10 eV [16]. An electron needs a lot of energy to overcome this wide gap and travel from valence to conductive band.

Semiconductors by their properties are between conductors and isolators. For instance, their band structure is similar to isolators, there is a band gap between valence and conduction, but it is possible for electrons overcome it[17].

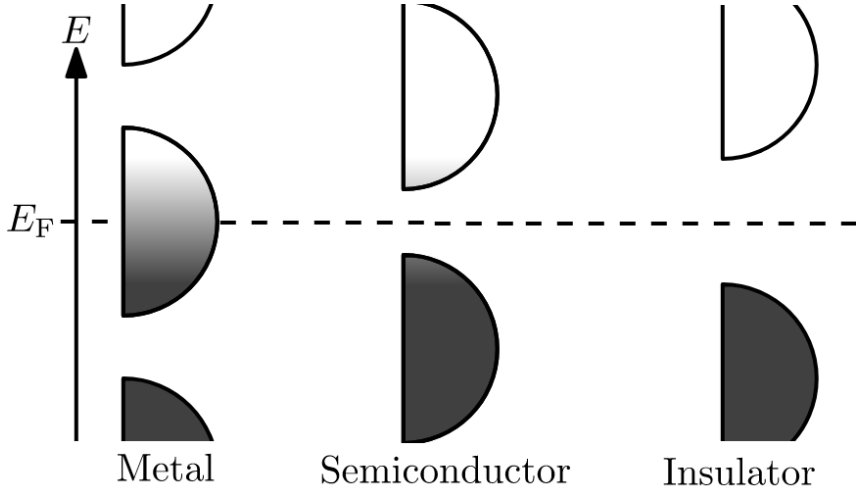

Fig. 1. The conduction and valence band configuration in metal, semiconductor and insulator[18]

Semiconductor can be organic or inorganic. Inorganic semiconductor is not carbon-based material, like silicon and gallium, that are in the majority of devices that people use: computers, tablets, smartphones, TVs, etc. These materials, Si, Ga or GaAs, has crystalline structure with strong covalent bonds, that are hard, fragile and with high melting temperature[17]. While organic semiconductors are more flexible, has amorphous structure and low melting temperature[19].

1.2. Organic semiconductors

Organic semiconductors are carbon-based materials with molecules consisting of conjugated systems, hydrocarbons with alternating single and double bonds. For example, in benzene molecular orbitals (MO) can be superposition of sp^2 and p_z orbitals. While sp^2 orbitals form σ bonds, p_z orbitals form delocalised electron cloud, π bonds. The overlap of sp^2 orbitals is higher than p_z orbitals, which results in higher energy splitting of binding σ and anti-binding σ*, compared to π and π*. The delocalised π system is responsible for electrical and optical properties, while σ bonds are strongest covalent bonds and determine mainly chemical bonds[19].

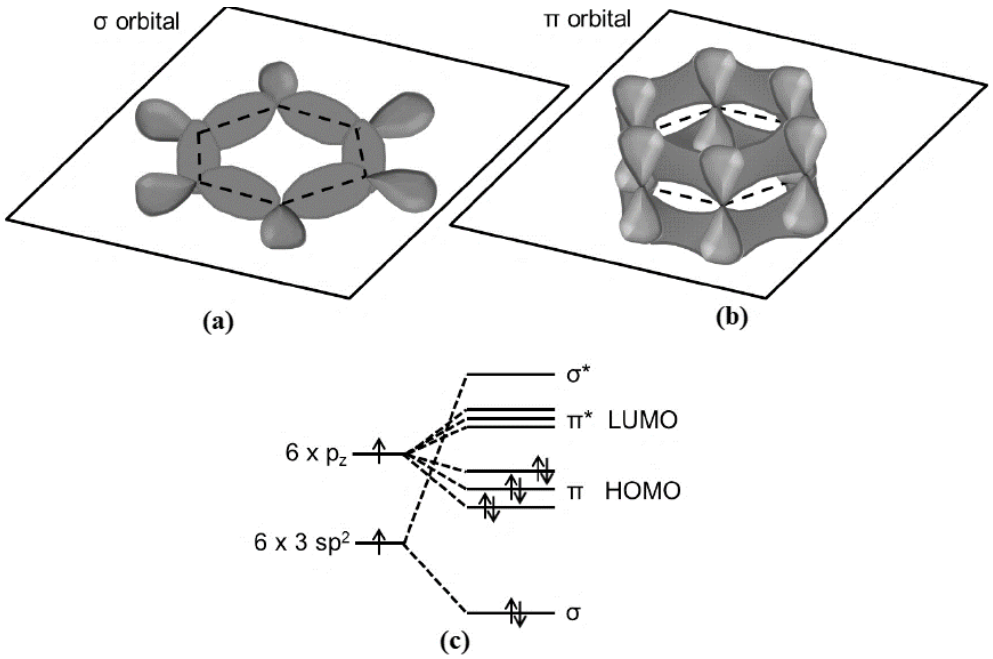

Fig. 2. Molecular orbitals of benzene ring and its energetic states[20]

The π and π* gives us Highest Occupied Molecular Orbital (HOMO) and Lowest Unoccupied Molecular Orbital (LUMO). The energy gap between HOMO and LUMO:

$$\Delta E = E_{LUMO} - E_{HOMO}; \quad (1)$$

here ΔE is molecules band gap. ΔE can be changed by adding additional aromatic rings, also by incorporating various atoms, such as oxygen, nitrogen, sulphur, etc. Therefore, these adjustments allow to design molecules with band gap from ultraviolet (UV) to infrared (IR) light. The HOMO and LUMO in organic molecules can be compared to valence and conductive bands in inorganic molecules[21] (figure 3).

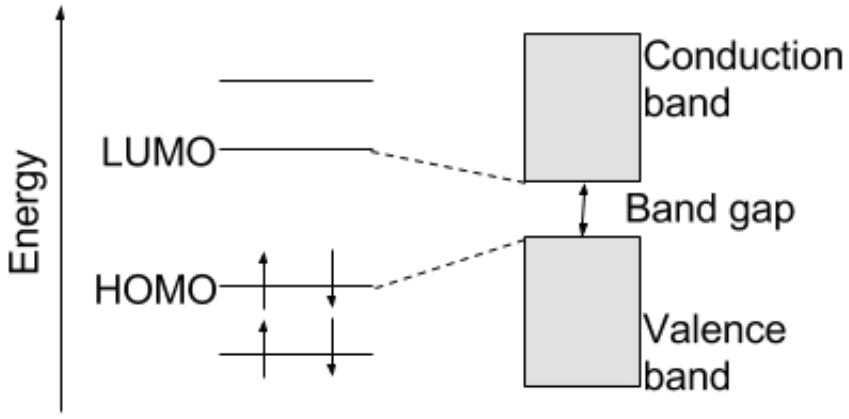

Fig. 3. Comparison of HOMO-LUMO levels in organic molecules and conduction-valence bandsin inorganic semiconductor[20]

1.3. Singlet and triplet state

In quantum mechanics singlet and triplet states are described as the spin of the system. It is a concept that characterizes particles angular momentum, not mechanical rotation. A singlet state refers to a system in which all the electrons are paired. Thus, the angular momentum of particles is zero and spin quantum number s is zero ($s = 0$). Only one spectral line of the system is shown in the spectrum. All molecules that are known exist in singlet state, except molecular oxygen that exist in triplet state.

In other case, triplet state has two unpaired electrons and its spin quantum number is equal to one (s=1). This means that there are three allowed values of spin components ($m_s = -1; 0; +1$). As a result the obtained spectral line will split into three lines, hence the name[22].

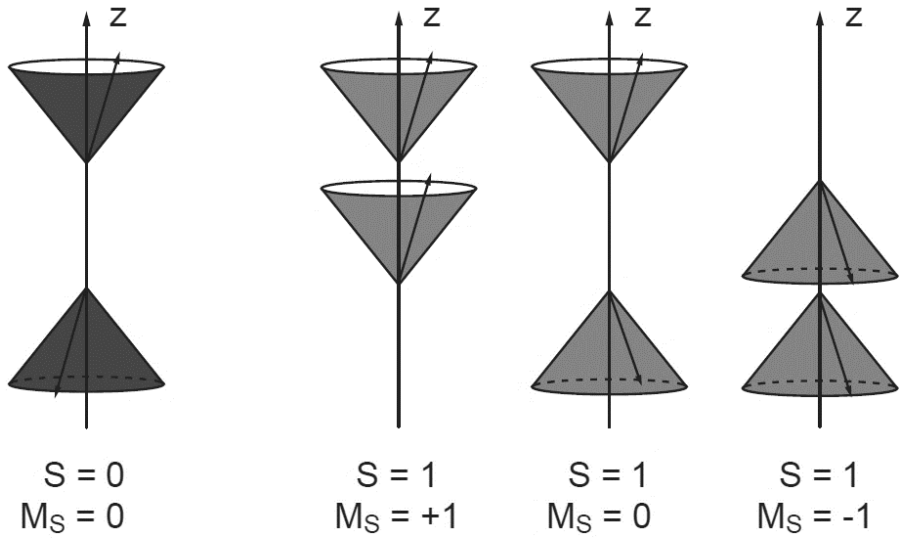

Fig. 4. spin configuration for singlet and triplet orbitals[23]

When organic molecule is excited, electrically or optically, a Coulomb bound pair of a negative charge electron and positive charge holes is formed, which is an electrically neutral exciton. These excitons in organic semiconductors are called Frenkel excitons[24]. They are bound to the molecule with binding energy 0.1–1 eV and are strongly localized. Whereas this is totally different than Wannier – Mott excitons in inorganic semiconductors, where excitons have binding energy of a few meV and the size in the order of tens of lattice constants[25].

Already mentioned that singlet has one state and triplet has three states. Therefore, exciton has the possibility to end in singlet state or one of three triplet states. So, for electrical exciton to take end at singlet or triplet state ratio is 1:3[24].

However, if the molecule is optically excited, there is transition from ground state S_0 to an excited state. Transition from the ground state to excited state requires spin conservation. That means excitons end in singlet state and transition to triplet state is forbidden. In quantum mechanics "forbidden" means that the probability of this transition happening is lower than of those which are not spin-forbidden. Thereby in organic molecules, exciting optically, the ratio of excited singlet-triplet states is 10^9:1 [26].

1.4. Jablonski diagram

Jablonski diagram is a widely used diagram, which explains light absorption-emission mechanisms in the system, usually in a molecule. It shows the position of the states, ground, excited singlet and triplet, also transactions that occur between them, for example, intersystem crossing and reverse intersystem crossing[27].

1.5. Franck – Condon principle

Absorption of a photon is instantaneous process. During light absorption, which happens in femtoseconds, electrons can move, but nucleus cannot. Therefore, there is no time for the atomic nuclei to readjust during the process of the absorption, so it moves after the process is over only rearrangement of electrons is involved, which are light compared to the nucleus. Specifically, this atomic nucleus readjustment, after absorption process is over, brings it to vibrational motion, energy release without occurrence of light emission. This process is called Frank – Condon principle. In figure 5 absorption and fluorescence is represented in a system with identical equilibrium geometry in ground and excited states. Most favourable transitions are the same transitions for both absorption and emission, 0-0 being the strongest. In that case, emission spectrum is a mirror image of the absorption spectrum, for this hypothetical organic molecule. Stoke shift is the shift of the fluorescence spectrum bands towards lower energy wavelengths compared to the absorption. The smallest displacement in equilibrium geometry of the excited state is because of the reorganization of the molecules in the medium[28].

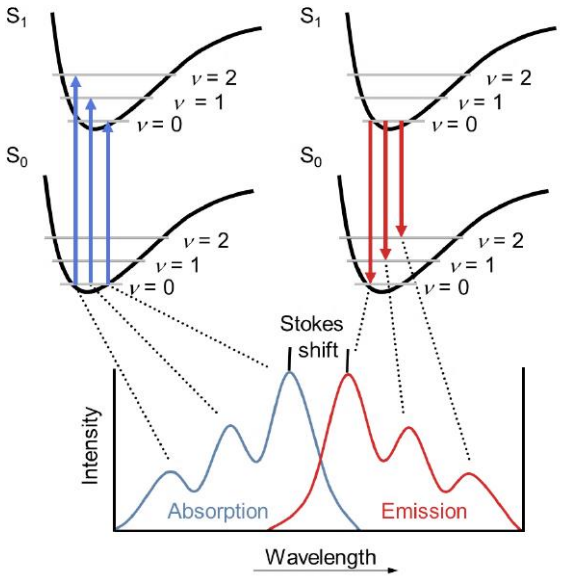

Fig. 5. Illustration of Frank-Condon principle where ground and excited states are in identical equilibrium geometry and absorption-emission spectra[29]

1.6. Quantum yield

The effectiveness of organic molecule emission is determined by quantum yield Φ. The differential definition of quantum yield reads:

$$\Phi = \frac{dn_E}{dt} \cdot \left[\frac{dn_A}{dt}\right]^{-1}; \quad (2)$$

here n_E is the number of the excited states and n_A is the number of photons absorbed. Alternatively, this formula can be used as photoluminescence quantum yield, which is the ratio of emitted photons and absorbed photons[30].

1.7. Fluorescence

One of the simplest mechanisms of light emission from the excited molecule to explain is fluorescence. The main principle is explained in Jablonski diagram in figure 6, where excitation is blue arrows up, fluorescence is green arrows pointing down and internal conversions is wavy yellow arrow down, when molecule is excited, electron goes from ground state S_0 to an excited singlet state S_n. Next, from S_n electron goes to S_1 by relaxing energy without emitting a photon (non-radiative vibrational pathway). Finally, when it reaches S_1, electron relaxes energy and travels back to ground state by emitting a photon. Fluorescence is very fast process, lasts approximately 10^{-9} s[31].

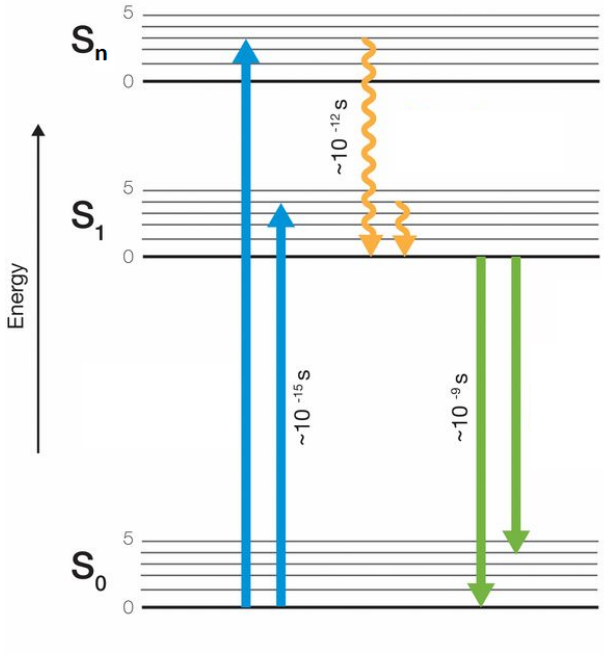

Fig. 6. Jablonski diagram of fluorescence emission mechanism[31]

Fluorescence has usual occurrence in nature, pigments with fluorescent properties can be found in some exotic fishes and corals.

1.8. Phosphorescence

The process of phosphorescence differs from fluorescence. For example, excited electron goes from ground state S_0 to S_n, then in non-radiative way travels to S_1. In phosphorescent molecules electron does not travel $S_1 \rightarrow S_0$. Because of heavy metal incorporation into the molecule weakens spin-orbit coupling, which leads to intersystem crossing (ISC) between singlet and triplet state. That means that electrons in the excited molecule travels from S_1 to the forbidden state, triplet T_1. Thus, during the intersystem crossing $S_1 \rightarrow T_1$ electron spin must be reversed. The transition from T_1 to ground state S_0, which is also a single state, requires spin reversal again (figure 7). As a result, spin reversal the energy relaxation is weaker and lasts longer, up to 1 s [32].

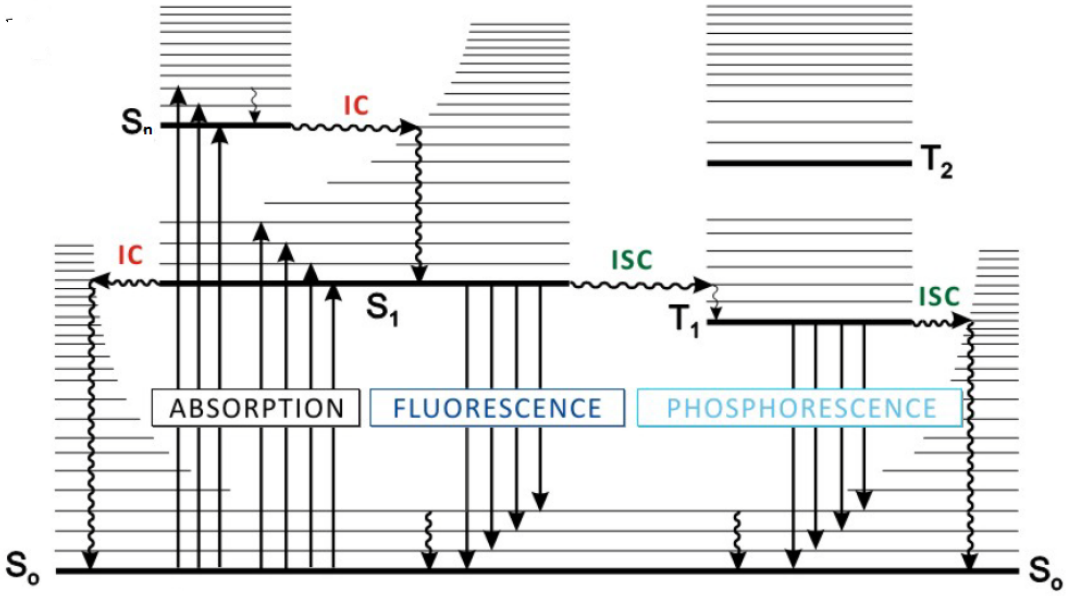

Fig. 7. Jabloski diagram of phosphorescence emission mechanism.[33]

1.9. Thermally activated delayed fluorescence

Thermally activated delayed fluorescence, more commonly known by its abbreviation TADF. This type of emission was known for almost a century since it was noticed by Perrin *et al.* back in 1929[34], but it was heavily investigated and explained in detail by Adachi et al in 2012[10]. One of the main properties that molecule should have, for TADF effect to occur, is formed charge transfer (CT) state. Notably, CT states occurs in molecules, that consist donor (D) moiety and acceptor moiety. D part of the molecule donates electrons, while A part accepts them. In the connection between D and A forms a charge transfer, transferring holes and electrons back and forth[35].

The principle of TADF is explained in figure 8. When molecule with D-A or D-A-D moieties is optically excited, the D part of the molecule absorbs energy and electron goes from S_0 to the locally excited singlet state of the donor S_1 (D). Because of D-A interactions CT state is formed, there is lower energy CT singlet state (CT_1) and electron transfers there. In competition with that, ISC can occur, and electron can travel from S_1 (D) to locally excited triplet state of the donor T_1 (D). These two processes compete. Now, the electrons in CT_1 can travel T_1 (D) by ISC process and harvest the triplets in that state. If the energy gap ($\Delta E_{S\text{-}T}$) between CT_1 and T_1 (D) is small and the thermal energy of the environment is sufficient, then reverse inter-system crossing process can occur (RISC). RISC process is when electrons transform from triplet state back to singlet state. Then from CT_1 electron relaxes its energy and delayed fluorescence occurs. Spin-flip processes between CT_1 and CT_3 are forbidden. TADF emitters are more efficient than fluorescence emitters, because of singlet and triplet harvesting. They are easier to design and synthesize than phosphorescence emitters, because they do not incorporate heavy metal atoms[36].

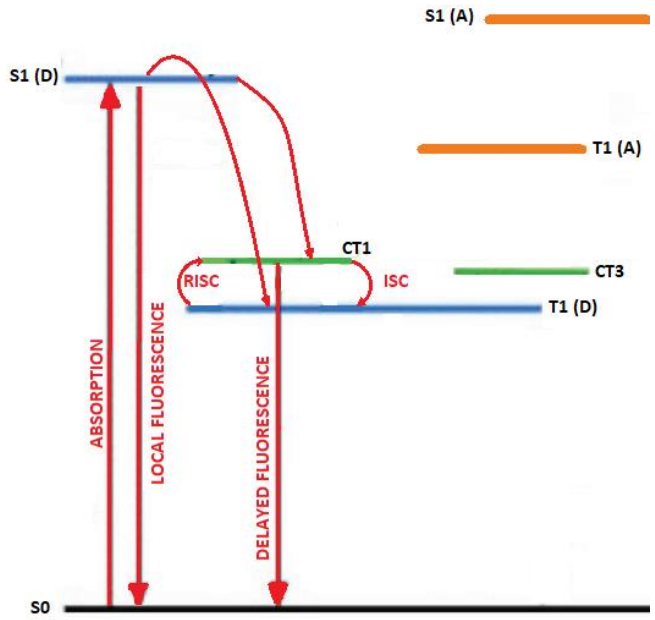

Fig. 8. Jablonski diagram representing thermally activated delayed fluorescence emission mechanism [36]

1.10. Intermolecular energy transfer mechanisms

Until now, only energy transfer mechanisms between molecule states were talked about. But it is important to talk about energy transfer mechanisms between molecules. In short, molecule can interact not just with itself or identical molecules, but also with different organic semiconductors. There are three major energy transfer mechanisms: reabsorption, Förster and Dexter energy transfer.

In a solid-state system consisting of D type molecules and A types molecules radiative energy transfer can occur. Energy can be transferred by emission and absorption process of a photon $h\upsilon$:

$$D^* \rightarrow D + h\upsilon\,; \tag{3}$$

$$A + h\upsilon = A^*; \tag{4}$$

here asterisk marks molecule being excited. Excited D molecule relaxes energy and emits a photon. That emitted photon gets absorbed by A molecule, that becomes an excited molecule[37].

Förster energy transfer is non-radiative energy transfer method. This method is based on energy transfer from D molecule to A molecule through dipole – dipole coupling. The mechanism of energy transfer is given in Jablonski diagram in figure 9. Donor molecule absorbs energy, which excites the molecule. Because of dipole-dipole coupling, the relaxed energy from donor molecule is transferred to acceptor molecule, where it can relax energy in a form of photon. Foster energy is given:

$$E_{Förster} = \frac{1}{1 + \left(\frac{r}{R_0}\right)^6}; \tag{5}$$

here (5) r is the distance between donor and acceptor molecules, and R_0 is the distance when energy transfer efficiency is reduced to 50%, also known as Förster radius. The length of this energy is 5 nm to 10 nm[38].

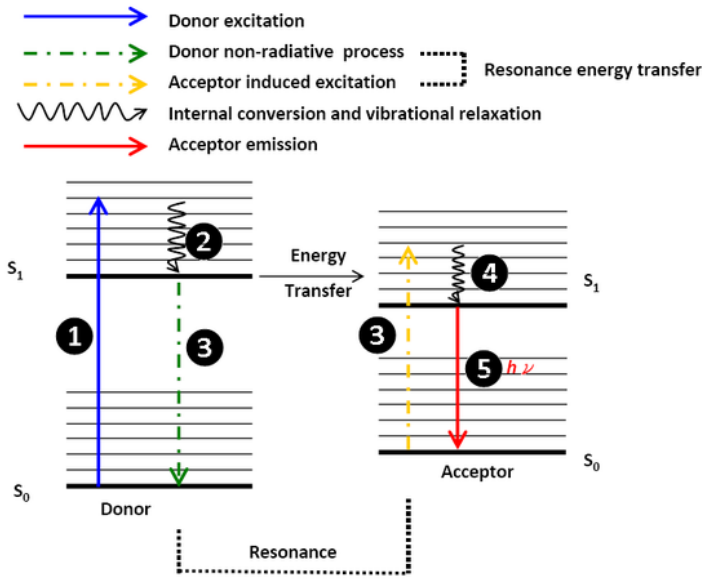

Fig. 9. Jablonski diagram showing simplified Förster energy transfer mechanism [38]

Because of the Coulombic dipole-dipole interactions, the total energy of each molecule has to be conserved. That means that triplet transfer from D to A is forbidden. But transfer from D singlet to A singlet or D singlet to A triplet is allowed:

$$D_S^* + A_S \rightarrow D_s + A_S^*; \quad (6)$$

$$D_S^* + A_T \rightarrow D_s + A_T^*; \quad (7)$$

In contrast with Förster energy transfer, where transfer is based on dipole-dipole coupling, Dexter energy transfer is based on electron exchange between neighbour molecules. For this transfer of electrons between molecules to occur, molecular orbitals of neighbouring molecules should overlap. That means, that the transfer distance is shorter than 1 nm. The mechanism of Dexter energy transfer is given in figure 9. Excited electron in D* molecule goes from S_0 to S_1. Because of MO of both D and A molecules are overlapping, the electron can transfer from D* S_1 to A S_1. Now A molecule has electron in the excited state. At the same time A gives an electron back from S_0 to D ground state[39, 40].

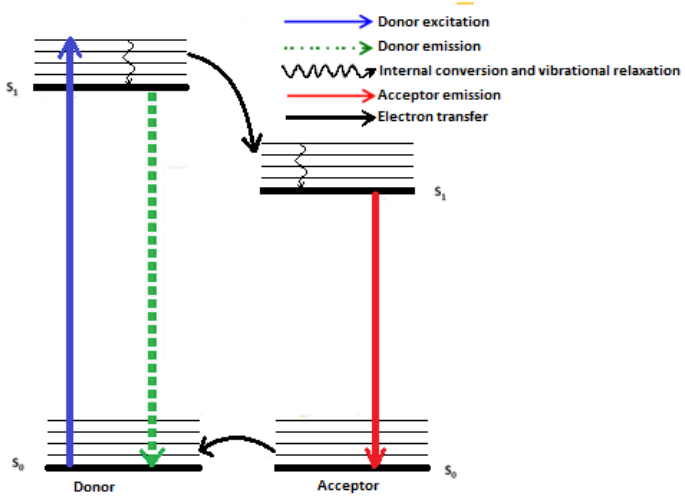

Fig. 10. Jablonki diagram showing simplified Dexter energy transfer mechanism[41]

Dexter transfer mechanism, based on Wigner-Witmer rule[42], requires total spin of the configuration to be conserved throughout the transfer process. So, the allowed transfers of the mechanism are:

$$D_S^* + A_S \rightarrow D_s + A_S^*; \quad (8)$$

$$D_T^* + A_S \rightarrow D_s + A_T^*; \quad (9)$$

1.11. Organic light emitting diode structure

The structure of organic light emitting diodes (OLEDs) evolved drastically since the first introduced OLED in 1987 by Tang and VanSlyke[6]. Their approach was to use Alq_3 [45] material as an emitting layer (EML) between two charge injection layers. Nowadays, to reach good volt-current, brightness and lifetime characteristics scientists and manufacturers use more complex structures. Emitting layers are the most important part of the OLED, but for it to emit light, charges need to recombine in that EML. That is why charge injection layers, hole injection (HIL) and electron injection (EIL), are used[46]. In most cases there is a large energy gap between HOMO-LUMO levels of EMT and charge injection layers. To balance this charge transport layers, hole transporting (HTL) and electron transporting (ETL), are used. By incorporating transporting materials with adjusted HOMO-LUMO levels, charges will reach recombination region smoothly[47]. By using materials with right charge mobility properties and thickness, charge recombination region can be shifted to the EML. To avoid exciton diffusion or charge leakage, which can cause broadening of recombination region, decreased efficiencies and colour impurities, charge blocking layers were started to use. Hole blocking layer (HBL) has appropriate HOMO-LUMO levels to let electrons pass to the EML and blocks transportation of holes. Vice versa situation is for electron blocking layer (EBL)[48]. From both sides of this OLED structure there are electrodes, cathode and anode. Whole structure is deposited on a solid transparent substrate, glass or polymer. The simplified structure and OLED working principle is given in figure 11. The charges are injected and travels towards EML, where holes and electron recombine to produce a photon. Furthermore, the materials can be used for more than one purpose, as an injection and transporting layer, or as transporting and blocking layer, to simplify the structure and enhance efficiency and stability[49].

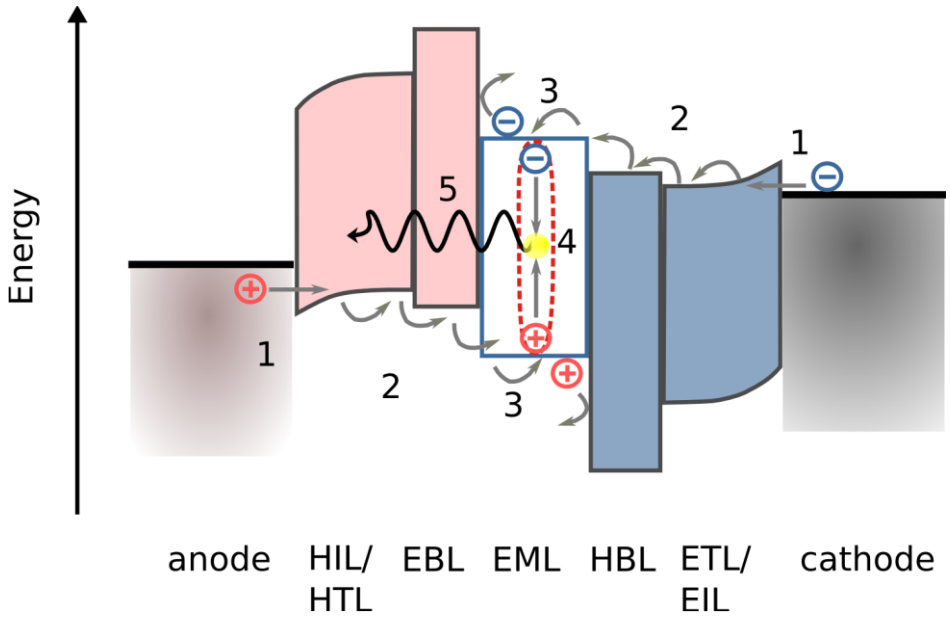

Fig. 11. Simplified structure of OLED device with showed recombination process principle[5]

1.12. OLED characteristics

Having OLED structure with balanced well designed structure and emitting material with great emission properties, leads to achieving great characteristics. The characterisation of OLED is based on a set of empirical standardised definitions. The luminous flux (measured in lumens) is total photometric power emitted in all directions from a light source. Whereas luminous intensity (measured in candela) is defined as luminous flux emitted into specific angle. This value takes into account the colour of the light and direction. Finally, the illuminance and luminance. It is defined as luminous flux and luminous intensity per unit of area, usually square meter, respectively[50].

The required typical brightness levels of light emitting device are given in figure 12.

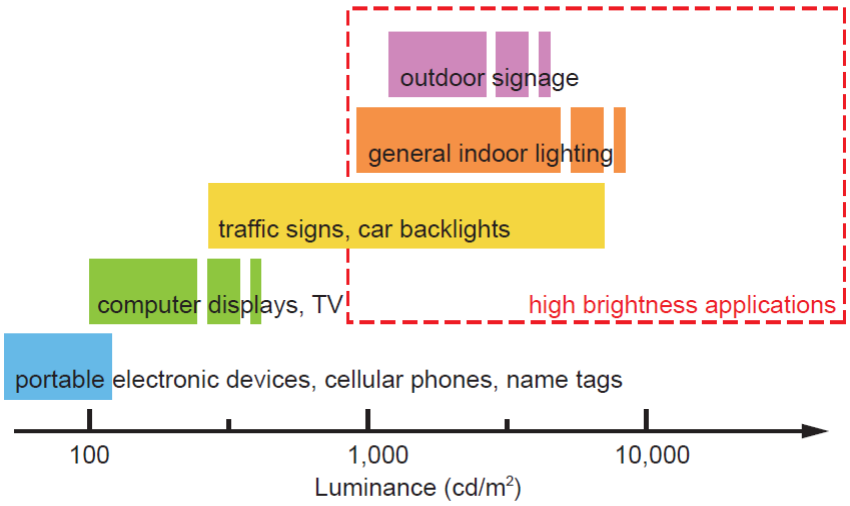

Fig. 12. Graph showing different brightness requirements for different applications[51]

Most important characteristic is OLED efficiency, which is composed of current efficiency power efficiency and quantum efficiency. Quantum efficiency can be separated into internal and external quantum efficiency (EQE). The later, *EQE*, is the most important of all mentioned.

Current efficiency (CE) describes amount of current flowing through devices emissive layer necessary to produce certain amount of luminescence[49]. The *CE* equation is as given:

$$\eta_{CE} = \frac{L}{J}; \tag{10}$$

Here (10) J is current density.

Power efficiency (PE) is characteristic described is the ratio of optical flux to the electrical input (11)[52]. The equation of *PE* is as given:

$$\eta_{PE} = \eta_{CE}\frac{f_D \pi}{V}; \tag{11}$$

Where V is applied voltage, η_{CE} is *CE* at the applied voltage and f_D is the angular distribution of emitted light in the hemisphere.

Internal quantum efficiency (IQE) is a value that describes the efficiency of light generation through charge recombination inside the device[53]. *IQE* depends on device structure and the photoluminescence properties of an emitter (12). The formula of *IQE* is as given:

$$\eta_{IQE} = \gamma * \eta_{ST} * \Phi_{PL}; \quad (12)$$

here γ is a value that is a fraction of injected carriers, that form exciton, which is a value that depends on the structure of the device. While η_{ST}, which is value that describes emitters ability to harvest excitons in singlet and triplet state, and $\Phi_{PL,}$ which is value of photoluminescence quantum yield, describes the ration between absorbed and emitted photons. The value of η_{ST} depends on the type of the emitter. As mentioned before, probability of excitons landing on singlet or triplet state is 1:3. Therefore, fluorescence emitters use only singlets, so the value η_{ST} would only be 0.25. However, phosphorescent and TADF emitters harvest excitons from triplet state, so there η_{ST} value can reach absolute 1[54]. The Φ_{PL} can be equal to 1 for all three types of emitters.

EQE takes in the account that light gets trapped inside of the device, so this value is concerned about the light that escapes[53]. That is why value of outcoupling efficiency η_{OUT} is taken into account:

$$\eta_{EQE} = \eta_{IQE} * \eta_{OUT}; \quad (13)$$

$$\eta_{EQE} = \gamma * \eta_{ST} * \Phi_{PL} * \eta_{OUT}; \quad (14)$$

EQE can be considered as the ratio of number of photons that escaped the device and number of charges that were injected (14).

1.13. Light outcoupling

The amount of light that escapes the OLED is limited. It is limited by optical interfaces of the materials characterised by different refractive indexes. This causes trapped modes inside of the device (figure 13). Simplified definition of outcoupling efficiency for the planar device, according to ray optics, can be written like this:

$$\eta_{OUT} = \frac{1}{2n_{glass}^2}; \quad (15)$$

here (15) n_{glass} is the refractive index of glass. The refractive index of standard glass is 1.51. Then η_{OUT} is equal 0.22. Need to note, that this value of outcoupling efficiency is applied only for standard planar bottom emitting OLED device. For different configuration OLED device this value may different[40].

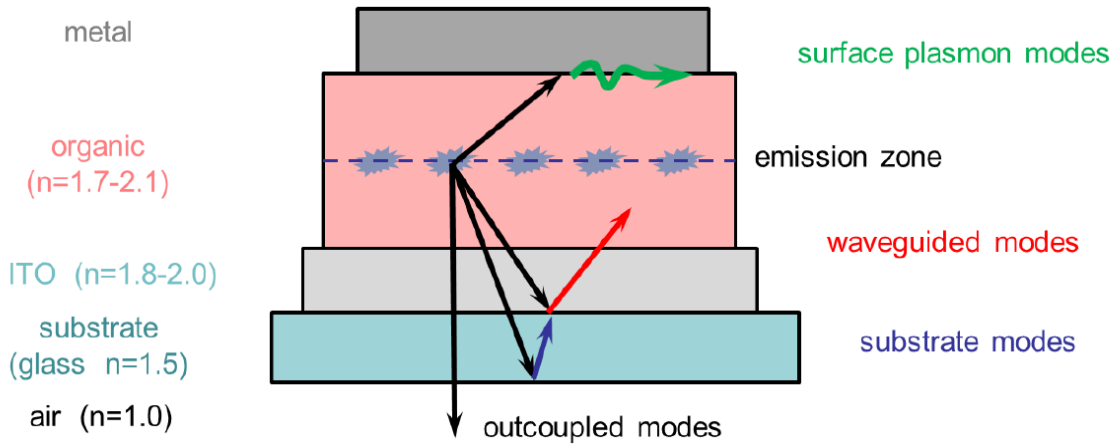

Fig. 13. Simplified process of how light gets trapped inside OLED device [55]

As mentioned, for different configurations the outcoupling efficiency can differ. That is why scientists try to extraction of light by incorporating additional layers, using different interface patterns or lenses, as it showed in figure 14[56].

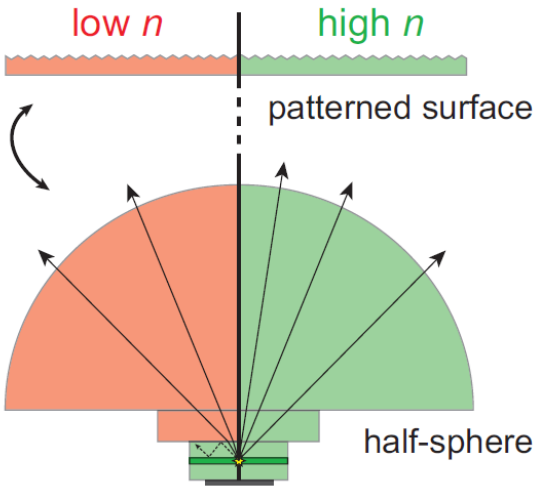

Fig. 14. Two possibilities of how to increase light outcoupling efficiency in OLED device, by using half-sphere lens or patterned surface [56]

1.14. Commission International d'Eclairage (C-I-E) coordinates

Humans perceives light colour and intensity from interpretation of two different cells that are in an eye's retina. Those cells are the cone and rode cell, respectively. The cone cells function well in bright conditions. The rod cell is more sensitive and easily saturates under intensive illumination. Cone cells, because they are not as sensitive to intensity of illumination, are sensitive to colour of the light. They are sensitive to three main wavelengths: blue, green and red, with a large overlap in between. Therefore, all colours that humans see, can be expressed as combination of those three main colours.

In general, any colour can be expressed by chromaticity coordinates x and y on the CIE diagram. The boundaries of this horseshoe type diagram contains colours of all the monochromatic light human eye can see (figure 15)[57].

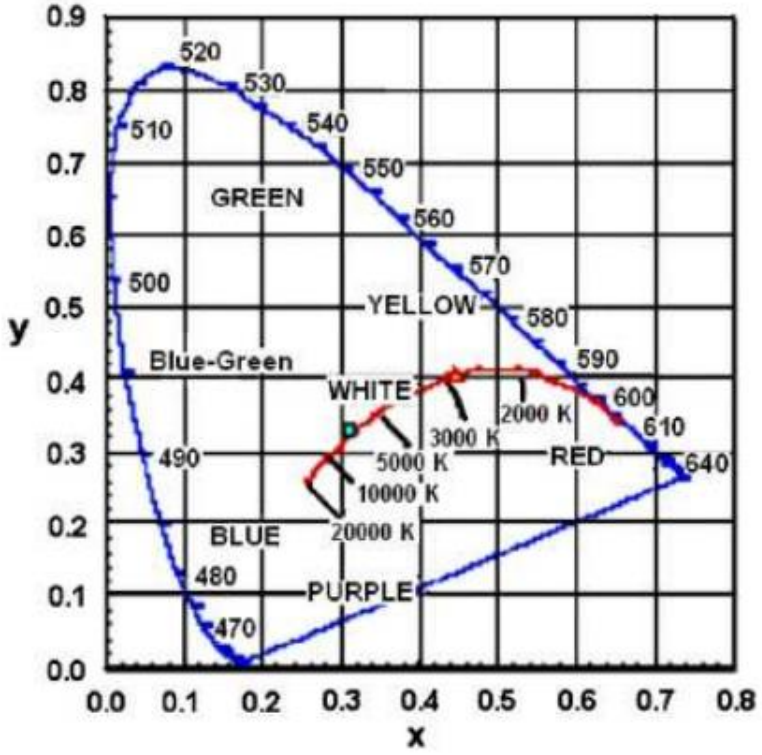

Fig. 15. CIE1931 diagram[57]

1.15. Organic sensors

It is not possible to imagine today's world without sensors. They are in almost every electronic device these days: from TVs, smartphones, to cars and smart fridges. A sensor is a device that responds to some stimulus by generating a functionally related output. Exposure to a certain analyte or change in ambient conditions alters one or more of its properties (e.g. mass, electrical conductivity, capacitance, etc.) in a measurable manner, either directly or indirectly. Main sensor characteristics[58] are:

- Accuracy defines how correctly the sensor output represents the true value
- Error is the difference between the true value of the quantity being measured and the actual value obtained from the sensor
- Precision is the estimate which signifies the number of decimal places to which a measurand can be reliably measured
- Resolution signifies the smallest incremental change in the measurand that will result in a detectable increment in the output signal. Resolution is strongly limited by any noise in the signal
- Sensitivity is the ratio of incremental change in the output of the sensor to its incremental change of the measurand in input.

Majority of sensors are made from inorganic materials. But organic materials as sensors getting a lot attention in past few years. They can offer many advantages, comparing to inorganic materials. They can be deposited on large area surfaces and at near room temperature. Also, they can be deposited on flexible support, like plastic or paper. This allows manufacture disposable sensors with cheaper roll-to-roll technology. The sensors properties can be adjusted by chemical synthesis, especially electronic properties (energy affinity and band gap)[59].

One of the ways organic semiconductors operate is their photophysical properties. For example, materials that exhibits room temperature phosphorescence. Because of how oxygen quench emission from triplet state, this type of materials can be used as oxygen sensing material[60]. Another application of organic materials is organic photo-sensors[61]. Typical camera sensors rely on silicon to trap photons and turn them into electrons. Fujifilm has pioneered the use of compounds to do the same job. By placing the photosensitive layer on top of the electronics, the organic sensor design is expected to reach a nearly 100% fill factor the percentage of the surface area sensitive to light — resulting in increased low-light sensitivity.

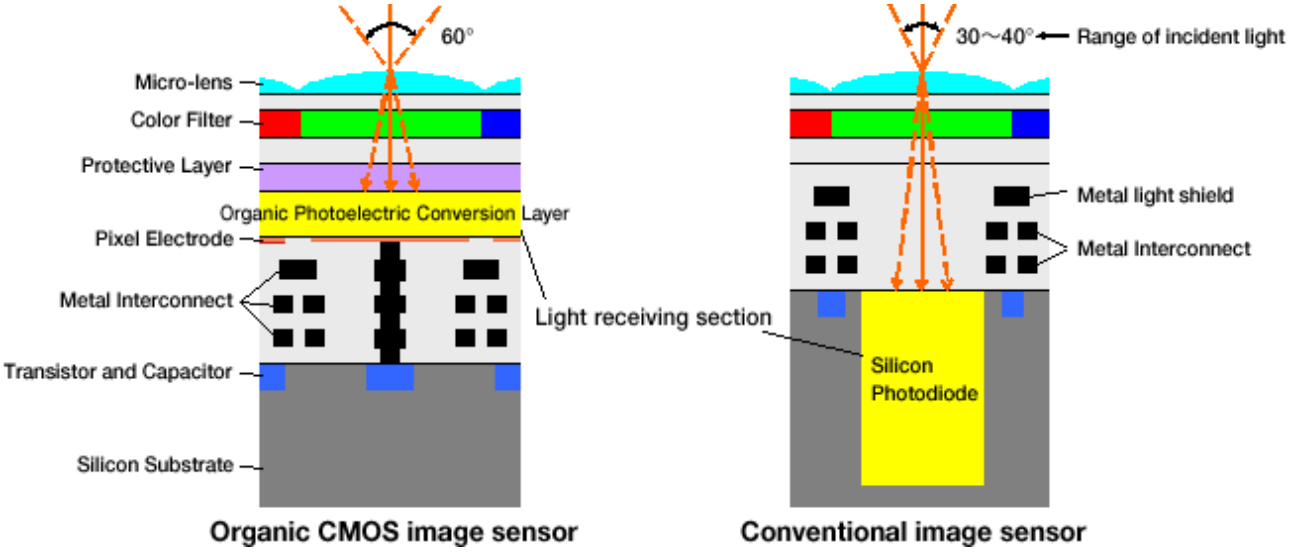

Fig. 16. Comparison between organic and silicon-based photo-sensor [61]

Taking in account that further generation of organic luminophores with enhanced or even unique properties can predictively leads to improvement efficiency of known optoelectronic devices or even to discovery of novel devices, two 5, 5-dioxi phenothiazine, benzophenone and sulfonyldi-4,1-phenylene based molecules (compounds 1 and 2) were selected as active materials for OLEDs and/or optical sensors in this work. Photophysical and electrochemical properties of the selected compounds 1 and 2 were characterized. Nature of emission of compounds 1 and 2 in different media were determined according steady-state and time resolved measurements at different temperatures. Photoluminescence properties of compounds 1 and 2 udder external stimuli such as UV excitation were investigated. Electroluminescent properties of compounds 1 and 2 as emitters in OLEDs were tested. Possible use of compounds 1 and 2 as active material of ultraviolet radiation dosimeters was explored.

2. Experimental section

2.1. Instrumentation

Providing photophysical measurements, materials were tested in solvent and solid state. Material concentration in a solution was 0.05 mg/ml. Then quartz cuvette filled with solution was used for absorption and emission measurements. For the UV treatment of the solvents a standard UV light source was used with 275 nm and 364 nm wavelength lamps. Solid state films on a glass substrate were deposited by using spin-coating technique with "Spin 150" (v=1500 rpm, a=250 rpm/s, t=50s). Spin-coater is integrated into "MBRAUN MB EcoVap4G" glove box, where inert atmosphere is maintained, O_2<10 ppm. For making solid state samples 2 mg/ml material solution was used. Glass substrates before deposition were cleaned with organic solvents, acetone, chloroform, and then cleaned UV ozone cleaner from "OSSILA". For PLQY measurements materials were vacuum deposited using "Kurt J. Lesker" vacuum chamber with two heaters for organic materials and two heaters for inorganic materials.

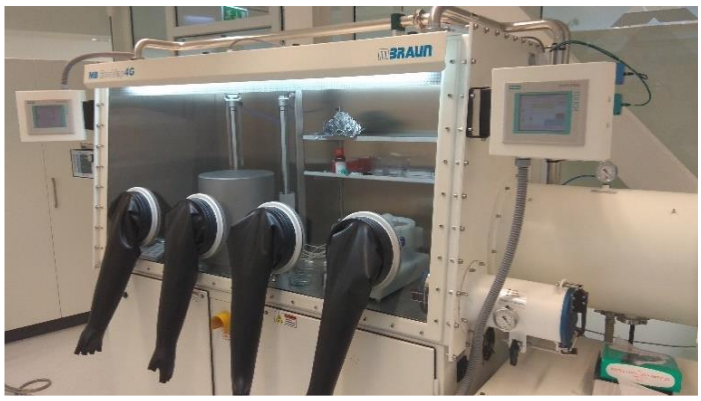

Fig. 17. "MBRAUN MB EcoVap4G" glowebox

Absorption measurements were done using "Avantes AvaSpec-2048XL" spectrophotometer, measurement range 200–1160 nm, 0.47 nm resolution, with symmetrical Czerny-Turner monochromator. Light source for absorption measurements was "AvaLight-DHc", which has deuterium lamp (emission range 200–500 nm).

a) b)

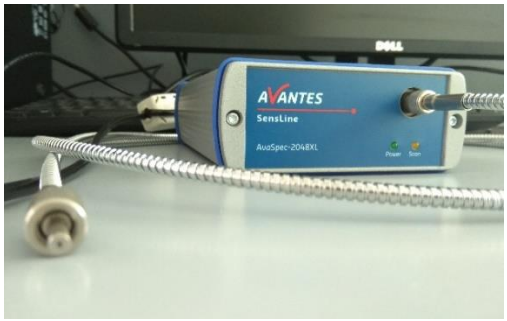

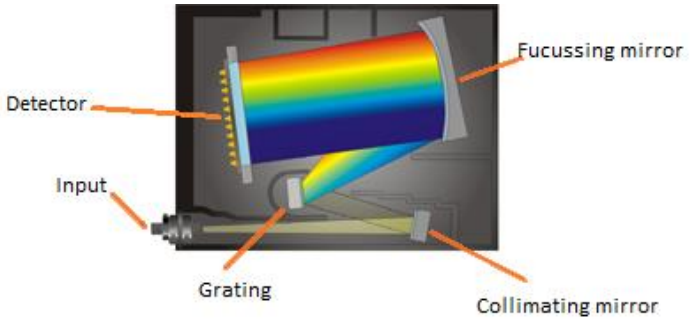

Fig. 18. a) "Avantes AvaSpec-2048XL" spectrophotometer, b) scheme of spectrophotometer

Additional photophysical measurements were done using "Edinburg Instruments FLS980" spectrometer. Light source used for measuring photoluminescence spectrum is xenon arc discharge lamp, emitting 230–1000 nm wavelength. The resolution of measured spectrum can be 0.05 nm. Single and double

grating Czerny-Turner monochromators are available in the FLS980 with 300 mm focal length, high optical throughput, excellent stray light rejection and low temporal dispersion. For photoluminescence life-time decay measurements "PicoQuant LDH-D-C-375" laser was used, λ = 374nm, maximum laser power 10 mW. The temperature depending measurement were done using "Oxford Instrument Optistat DN2" cryostat. The PLQY measurements were done using integrated sphere.

a) b)

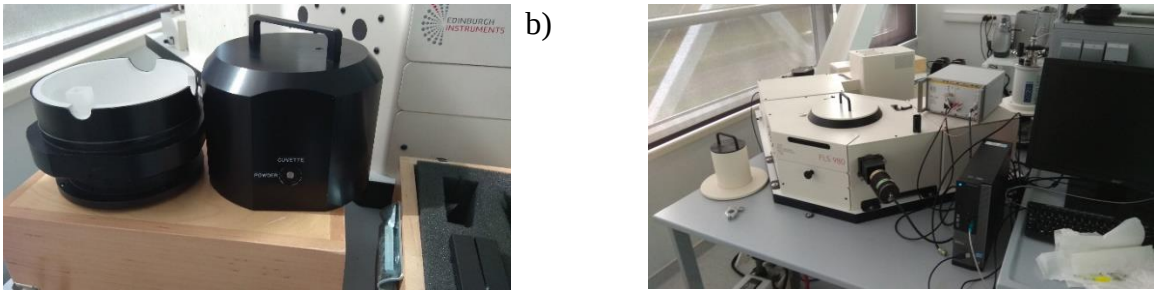

c) d)

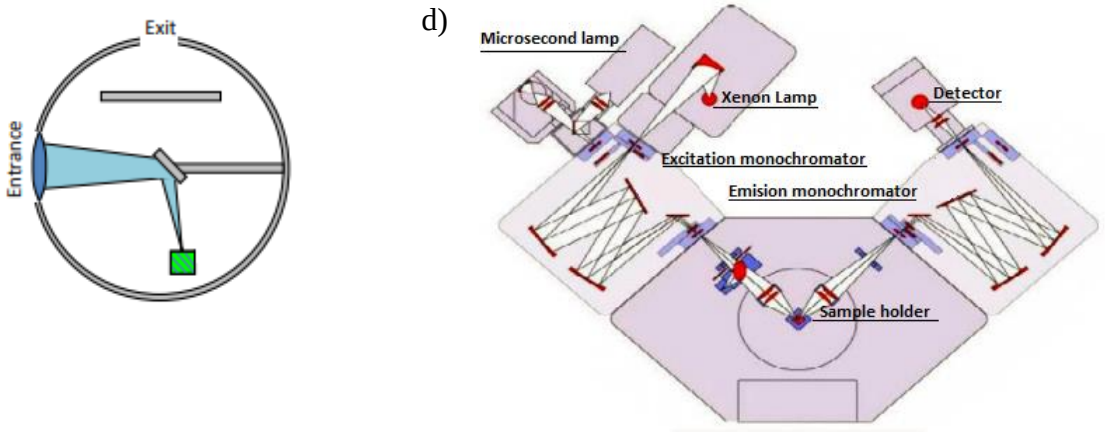

Fig. 19. a) sphere used for PLQY measurements, b) spectrometer "FLS980", c) working principle of PLQY sphere, d) working principle of spectrometer

Sensitivity measurements were done using a homemade set-up, consisting of UV lamp (275 nm) and silicon photodiode PH100-Si-HA-D0t, which are in a box. The cuvette with solution and detector was at the same distance from UV source, the power of UV light is measured. After the power is known, the solution is treated with UV light for 10 min. After the treatment was done, photoluminescence spectrum was measure. After the measurement new solution was used and placed together with detector closer to the UV lamp.

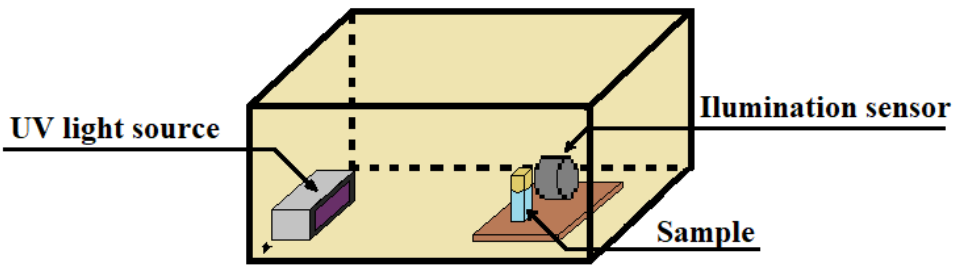

Fig. 20. Simplified scheme of setup used for sensitivity measurements

Molecules crystallographic analysis was done by using "Rigaku XtaLab" mini diffractometer. X-ray source was graphite monochromated Mo Kα (λ = 0.71075 Å). Measurements were done at room temperature.

To determine energies of ionisation potential and electron affinities cyclic-voltammetry (CV) measurements were done. CV measurements were done with glassy carbon working electrode in three electrode cell. Measurements of dry room temperature 0.1 M tetrabutylammonium hexafluorophosphate ($TBAPF_6$) solvent (as the electrolyte) were performed using "EcoChemie Autolab PGSTAT20" potentiostat under nitrogen atmosphere. Experiments data was collected using "General Purpose Electrochemical System" software. Electrochemical cell consists of three electrodes: platinum wire and platinum coil as working electrode and auxiliary electrode respectively and Ag wire, which is reference electrode calibrated for ferrocene redox. Potential rate was 50 mV/s. Ionisation potential was calculated from onset oxidation potential by using relationship:

$$\mathrm{IP} = E_{ox}^{onset} + 4.8 \tag{16}$$

Electron affinity was calculated using the onset reduction potential:

$$\mathrm{EA} = E_{red}^{onset} + 4.8 \tag{17}$$

For device preparation organic layers were vacuum deposited on glass substrate coated with indium-tin-oxide (ITO). ITO glass substrates, with sheet resistivity of 15 Ω/sq, were patterned using zinc dust and hydrochloric acid (HCl). Using "Kurt J. Lesker" vacuum chamber, which is integrated in the glovebox organic and metal layers were deposited. The depositions were done under $2x10^{-5}$ mbar pressure. Shutter protects samples from unwanted depositions. To ensure uniform deposition, sample holder is rotating throughout the process. The temperature of organic and metal evaporators is controllable.

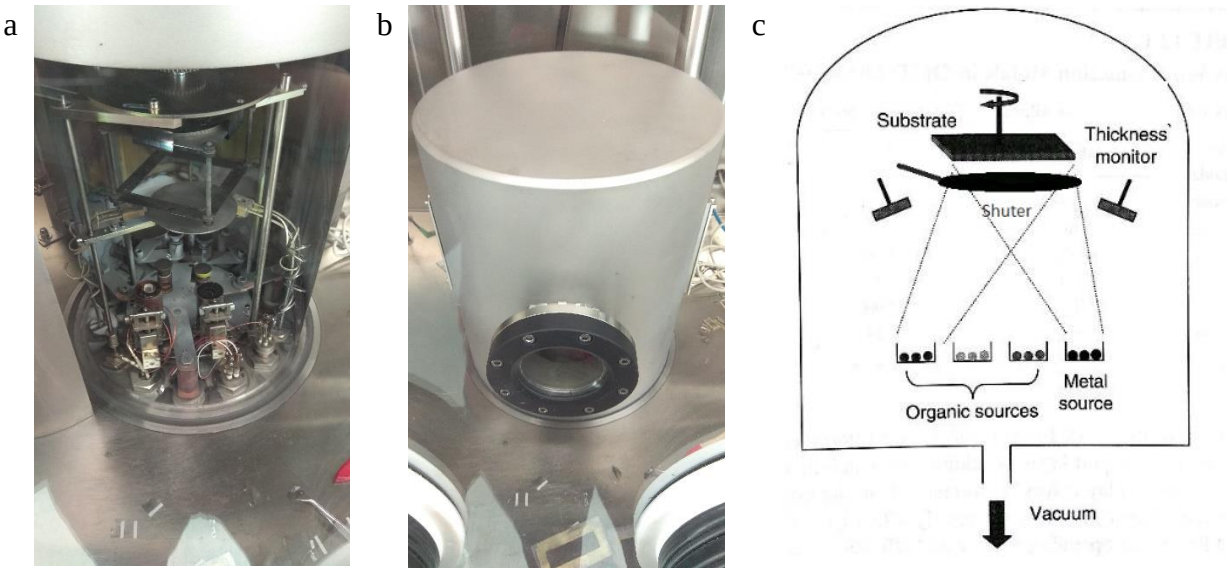

Fig. 21. a) and b) "Kurt J. Lesker" evaporation chamber used for organic materials and metal deposition, c) schematics of the evaporation chamber

Device characteristics, such as current density–voltage and luminescence intensity–voltage, were recorded using Keithley 6517B electrometer, calibrated silicon photodiode PH100-Si-HA-D0 together with the Keithley 2400C source meter. Electroluminescence spectrum dependence on voltage was

measured using AvaSpec-2048XL spectrometer. Device efficiencies were calculated with "MatLab" program, using luminescence, current density and electroluminescence characteristics. CIE 1931 coordinates were calculated and plotted on CIE 1931 colour scheme using "MatLab" program.

2.2. Materials

In this work two materials were investigated. First material is bis[4-(5,5-dioxo-10H-phenothiazin-10-yk)phenyl]methanone (1) and second is 10,10'-(sulfonyldi-4,1-phenylene)bis-10H-phenothiazine-5,5-dioxide. Both molecules, 1 and 2, are symmetrical, have the same moiety on the sides, 5,5-dioxo-10H-phenothiazine. Difference is between 1 and 2 is moieties that connects dioxo-phenothiazine. While in molecule 1 the middle part is benzophenone, in molecule 2 it is sulfonyldi-4,1-phenylene.

Materials 1 molar mass is 648.79 g/mol and material 2 molar mass is 684.84 g/mol. Materials were designed and synthesized by Edgaras Narbutaitis in Kaunas University of Technology.

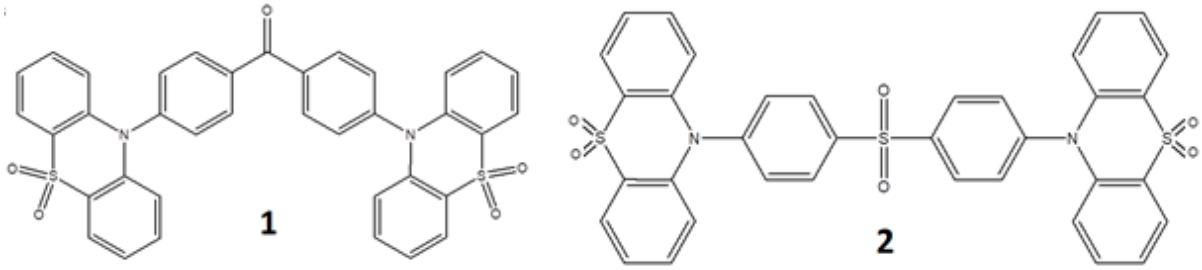

Fig. 22. Chemical structure of materials 1 and 2

For solvatochromism measurements different solvents were used: toluene, σ-xylene, chloroform, tetrahydrofuran, N, N- dimethylformamide and acetonitrile. Solvents has different dielectric constants and different orientation polarizability (table 1). All the materials were commercially available.

Table 1. Characteristics of used solvents

Solvent	**Dielectric constant *ε***	**Refractive index *n***	**Orientation polarizability *Δf(ε, n)***
Toluene	2.38	1.49	0.014
σ-Xylene	2.57	1.505	0.027
Chloroform	4.81	1.44	0.149
Tetrahydrofuran (THF)	7.58	1.41	0.210
N, N- dimethylformamide (DMF)	37	1.43	0.284
Acetonitrile	37.5	1.344	0.30

In table 1 the values of orientation polarizability Δf is presented, those values are calculate using dielectric constant and refractive index:

$$\Delta f = \frac{\varepsilon - 1}{2\varepsilon + 1} - \frac{n^2 - 1}{2n^2 + 1} \tag{18}$$

Materials used in device preparation are showed in figure 22 and their characteristics are given in table 2.

Table 2. Characteristics of materials used in device manufacturing

Materials	**Chemical name**	**Purpose**	***HOMO*, eV**	***LUMO*, eV**
MoO3 [62]	Molybdenum Oxide	HIL	-5.3	-2.3
C70[63]	[5,6]-Fullerene-C70	HTL	-6.1	-4.2
mCP[64]	9,9-(1,3-phenylene)bis-9H-carbazole	EBL	-6.1	-2.4
TSPO1[65]	Diphenyl[4-(triphenylsilyl)phenyl]phosphine oxide	HBL	-6.8	-2.5
TPBi[66]	2,2′,2"-(1,3,5-Benzinetriyl)-tris(1-phenyl-1-H-benzimidazole)	ETL	-6.2	-2.7
LiF[67]	Lithium fluoride	HIL	-3.7	

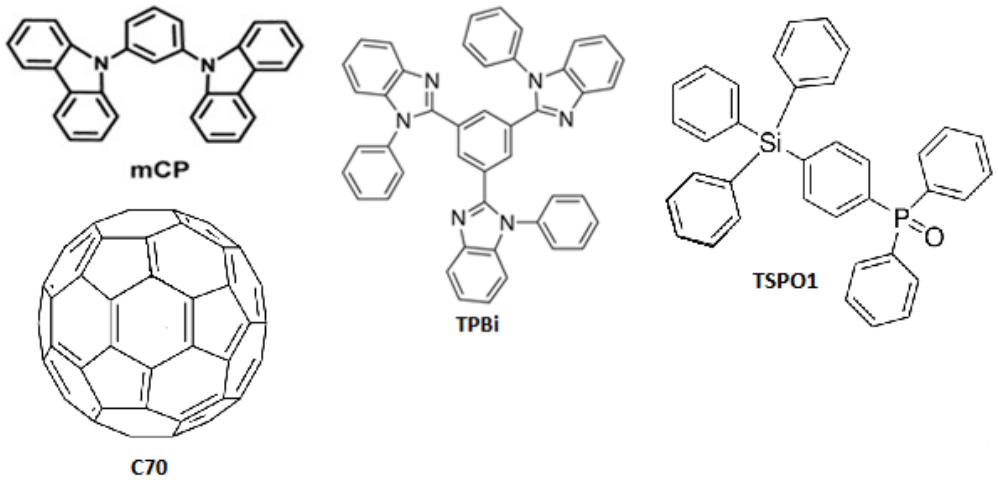

Fig. 23. Chemical structure of materials used in device manufacturing

2.3. Device structure

The structure of the devices with material 1 or 2 as EML was MoO_3(0.2 nm)/ C70(40 nm)/ mCP (4 nm)/ EML (20 nm)/ TSPO1 (4 nm)/ TPBi (40 nm)/ LiF (0.3 nm)/ Al (figure 24)

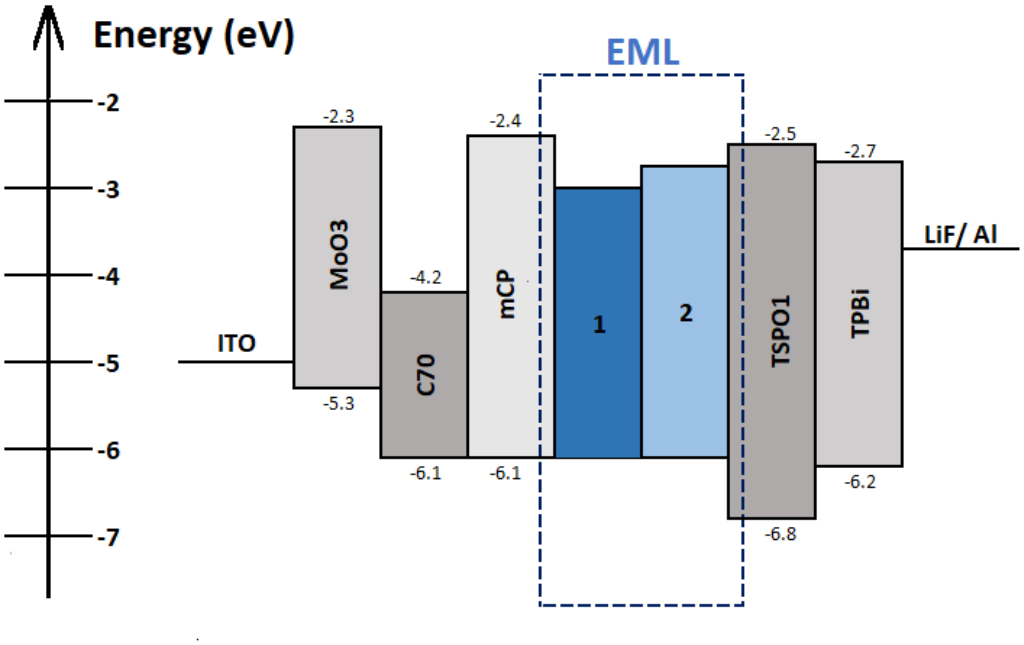

Fig. 24. Simplified structure of manufactured OLED devices

3. Results and discussion

To find most appropriate applications in optoelectronic devices for the selected compounds 1 and 2, their photophysical, electrochemical and electroluminescent properties were deeply investigated as described below.

3.1. Photophysical measurements

The UV absorption spectra of different solutions were recorded (figure 25) and in both cases, material 1 and 2, there were absorption maxima at 300, 320 and 328 nm. These maxima can be attributed to $\pi \rightarrow \pi^*$ transitions of 5,5-dioxide phenothiazine. Furthermore, these energy bands were not reacting to the change of the solvent polarity. But, in absorption spectra of material 1 there is a low energy band, in 340–370 nm range, which was sensitive to solvent polarity (figure 25a). This energy band can be attributed to the formation of CT state between 5,5-dioxide phenothiazine and benzophenone moieties. However, formation of CT state was not noticed in material 2.

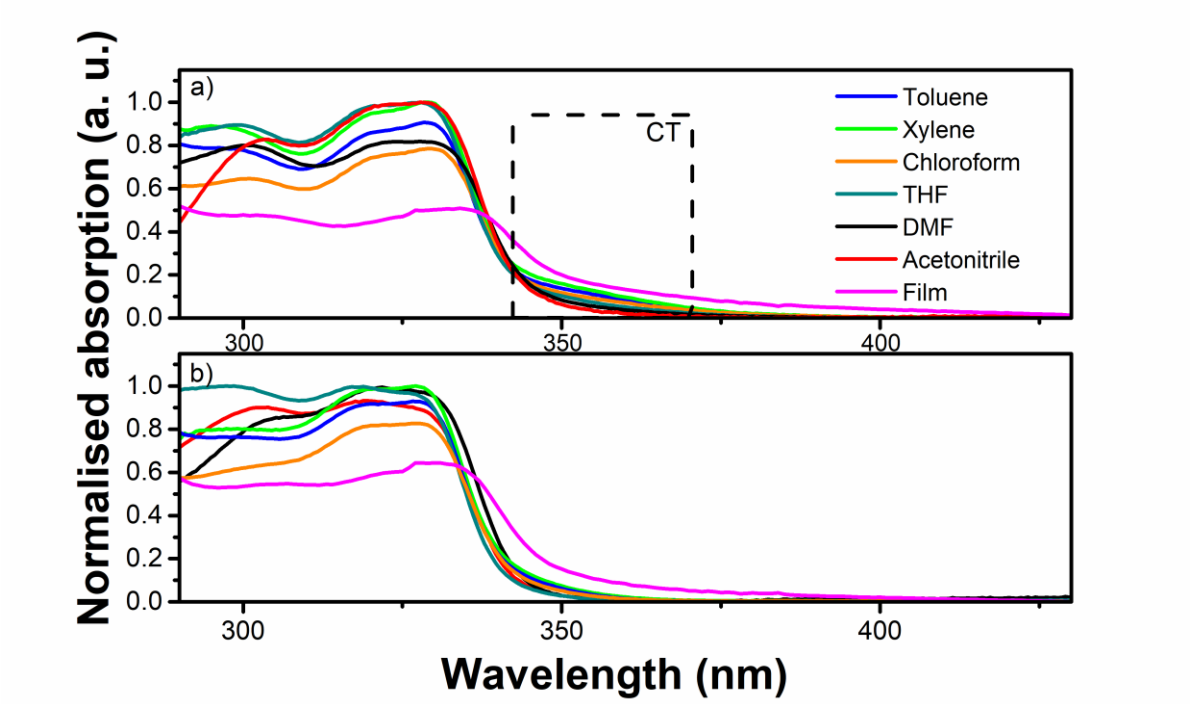

Fig. 25. Absorption spectra dependence on solvent of a) compound 1 and b) compound 2

Even though CT state formation in absorption spectra is not visible for material 2, the emission spectra shows positive bathochromic shift for materials 1 and 2. These bathochromic shifts can be attributed to formation of CT state. Knowing that polarity of the solvent affects CT, the PL emission redshifts.

Comparing PL spectra of different polarity solutions, from toluene, which is considered non-polar, and acetonitrile, which is polar, it is obvious that that PL emission of material 1 shifts from 416 nm (toluene) to 535 nm (acetonitrile) and the difference between spectra maxima is 119 nm. The same situation for material 2, were the difference between these two solutions is 45 nm. The large shift of PL spectra indicates strong CT formation.

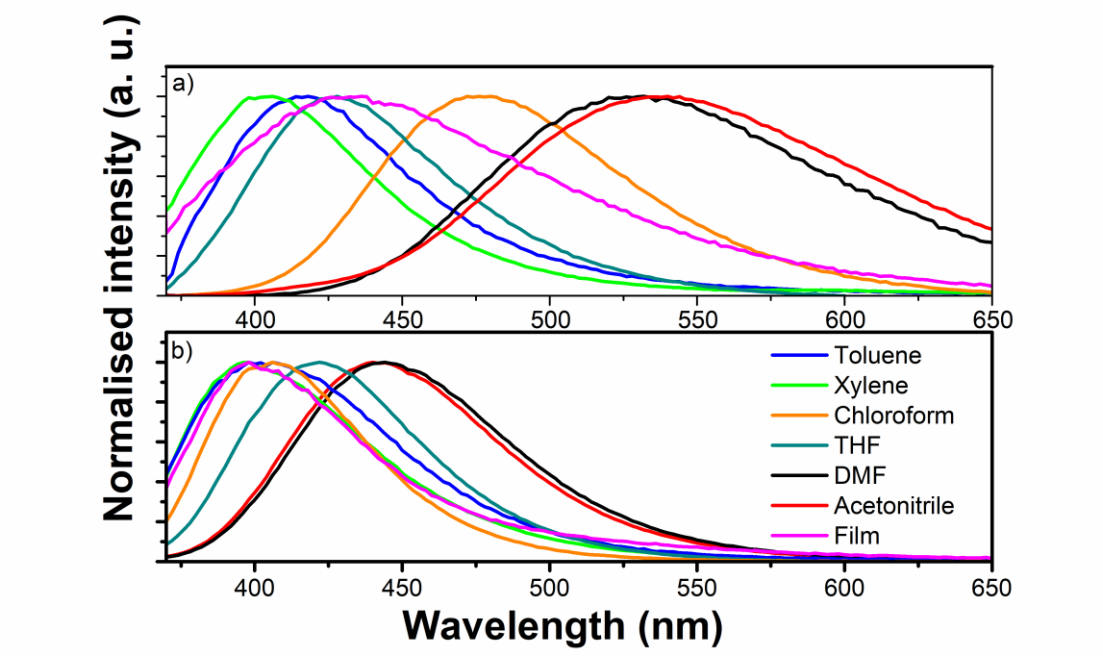

Fig. 26. PL spectra dependence on used solvent of materials a) 1 and b) 2

Because of different CT energies in different solvents, different Stoke shifts ($\Delta\upsilon = \upsilon_{abs}$-$\upsilon_{em}$) were obtained in different solutions. For example, Stokes shifts of 6390 and 5470 cm^{-1} were obtained for toluene solutions, and 11800 and 7760 cm^{-1} of acetonitrile solutions of 1 and 2 respectively. Different slopes of Lippert–Matagga plots were obtained, 19860 and 8895 cm^{-1}, for material 1 and 2 respectively (figure 27). The 19860 cm^{-1} slope of material 1 shows strong CT character, in comparison is among the highest of donor-acceptor type TADF emitters[68].

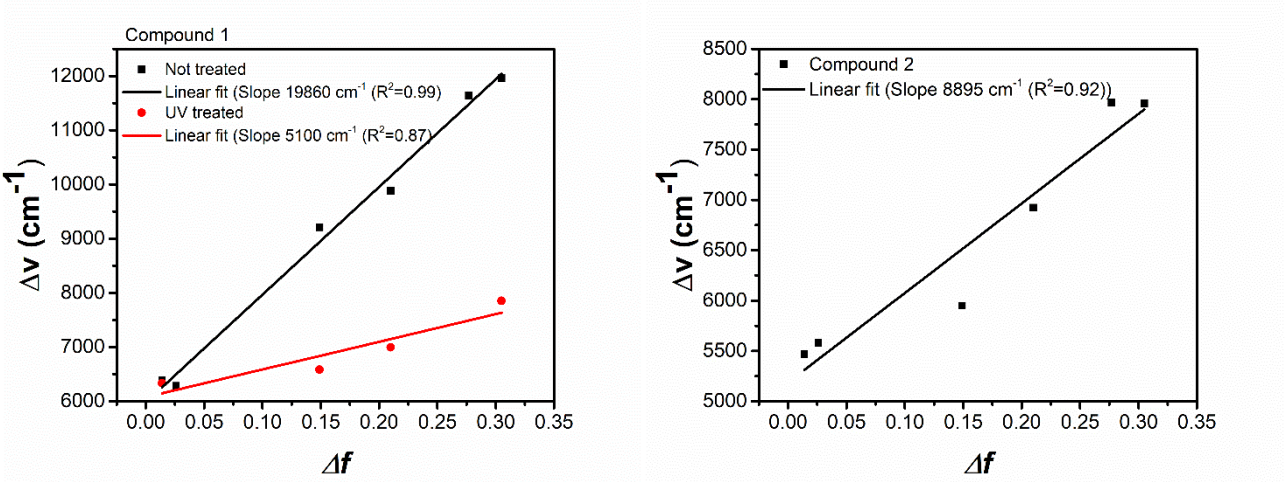

Fig. 27. Lippert–Matagga plots of a) Non-treated and UV treated material 1, b) material 2

To investigate if triplet state was incorporated in the emission mechanism, the solution of toluene was degassed with inert gas. As it showed in figure 28 a and b, after degassing toluene solution the PL emission intensity increased by 6 and 2.6 times for materials 1 and 2, respectively. The PL emission decays of toluene solutions did not drastically change. The delayed fluorescence component got a little bit longer after removing oxygen from toluene solution of 1 (figure 287 c). For comparison, there is obvious increasement of delay component after degassing much polar acetonitrile solution of compound 1. The same situation is for material 2 (figure 28 d). After degassing toluene solution there

is no obvious change in PL emission decay graph, but there is longer delay component after degassing acetonitrile solution.

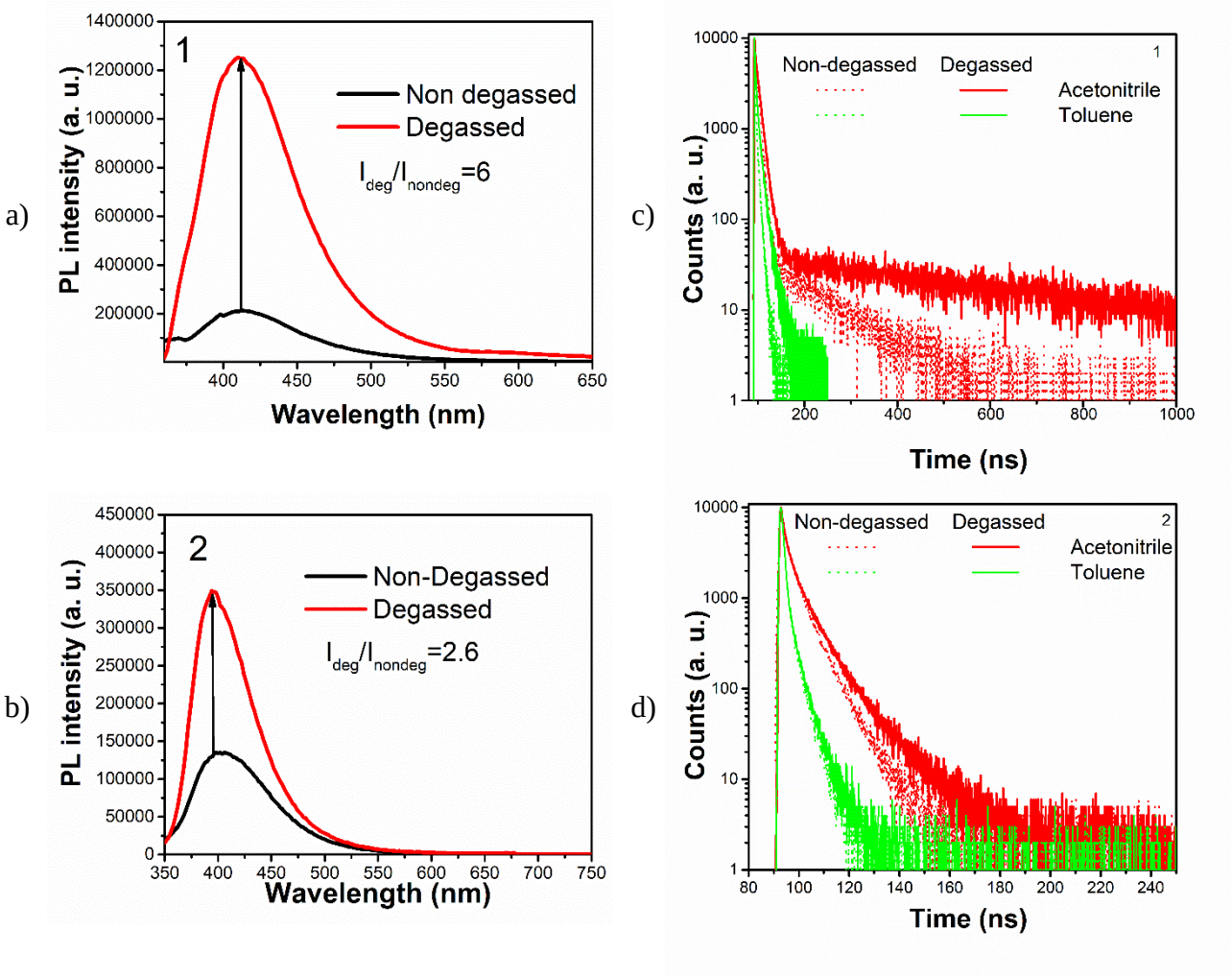

Fig. 28. a) material 1 solution in toluene PL intensity dependence on oxygen, b) material 2 solution in toluene PL intensity dependence on oxygen, c) material 1 solution in toluene and acetonitrile PL decay dependence on oxygen, d) c) material 1 solution in toluene and acetonitrile PL decay dependence on oxygen

Even though that there the triplet state is used in the photoluminescence, the gap between singlet and triplet levels are quite big. The ΔE_{ST} in THF solution at 77 K of material 1 and 2 was 0.49 eV and 0.32 eV, respectively (table 3). Large ΔE_{ST} can be a problem for effective RISC to be carried out.

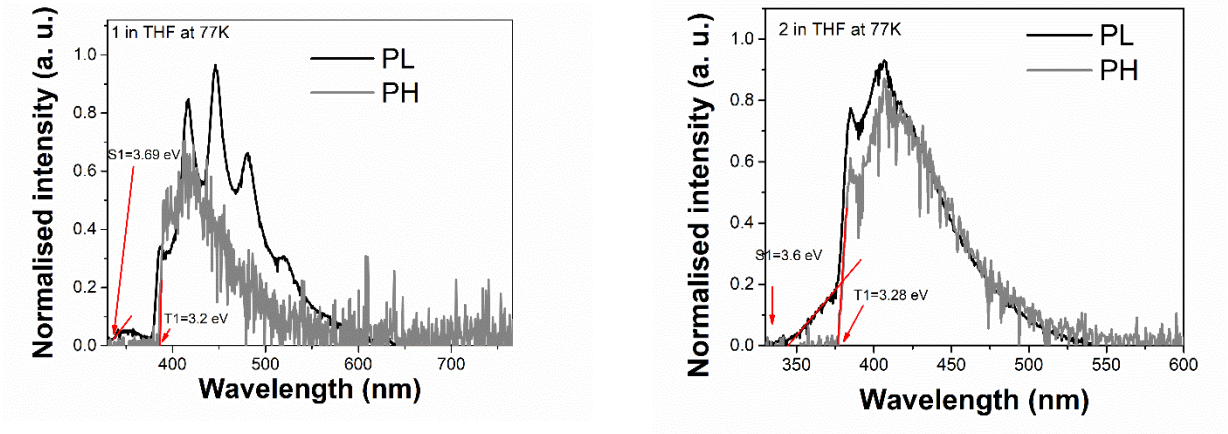

a) b)

Fig. 29. PL and PH spectra at 77K of a) 1 in THF solution, b) 2 in THF solution

Absorption spectra of films 1 and 2 were only slightly red-shifted in comparison to their spectra in solutions, showing the same shapes of low-energy bands (Figure 25). These films emitted blue light under UV excitation in range from 300 nm to 340 nm having one–banded PL spectra with maximum at 432 and 397 nm, respectively (Figure 26).

The PLQY of toluene solutions of 1 and 2 were 1.8% and 14.2% respectively. After application oxygen removal correction factor (I_{deg}/I_{nondeg}) the *PLQY* was 10.8% and 36.9% for toluene solution of 1 and 2 respectively. Furthermore, the *PLQY* for solid-state films were 7.4% and 9.3% for 1 and 2 respectively (table 3). The solvatochromic effect and incorporation of triplet state leads to a conclusion, that compounds 1 and 2 can be characterised by thermally activated delayed fluorescence behaviour.

Table 3. Photophysical and electrochemical properties of studied materials

Material	λ_{tol}, **nm**	λ_{film}, **nm**	$I_{deg}/I_{non\ deg}$	E_g^{opt}, **eV**	ΔE_{ST}, **eV**	IP^{CV}, **eV**	EA^{CV}, **eV**	E_g^{CV}, **eV**	$PLQY_{tol}^*$, **%**	$PLQY_{film}$, **%**
1	416	432	6	3.1	0.49	6.1	3	3.1	1.8/10.8	7.4
2	397	400	2.6	3.3	0.32	6.1	2.8	3.3	14.2/36.9	9.3

**PLQY* values in air and with applied correction factor

3.2. Electrochemical measurements

The electrochemical characteristics, *IP* and *EA*, of solutions with materials 1 and 2 are given in Table 3 and CV curves are in figure 30. The values from CV curves were calculated from the onset potential of first oxidation after calibrating against ferrocene. The *IP* values for both material 1 and 2 were 6.1 eV. The *EA* values were calculated from onset of first reduction process after calibrating against ferrocene. These values for 1 and 2 were 3 and 2.8 eV respectively. The band gap of materials 1 and 2 between calculated *IP* and *EA* values is 3.1 and 3.3 eV respectively. The same band gap values were estimated from optical measurements, onset of the absorption spectrum.

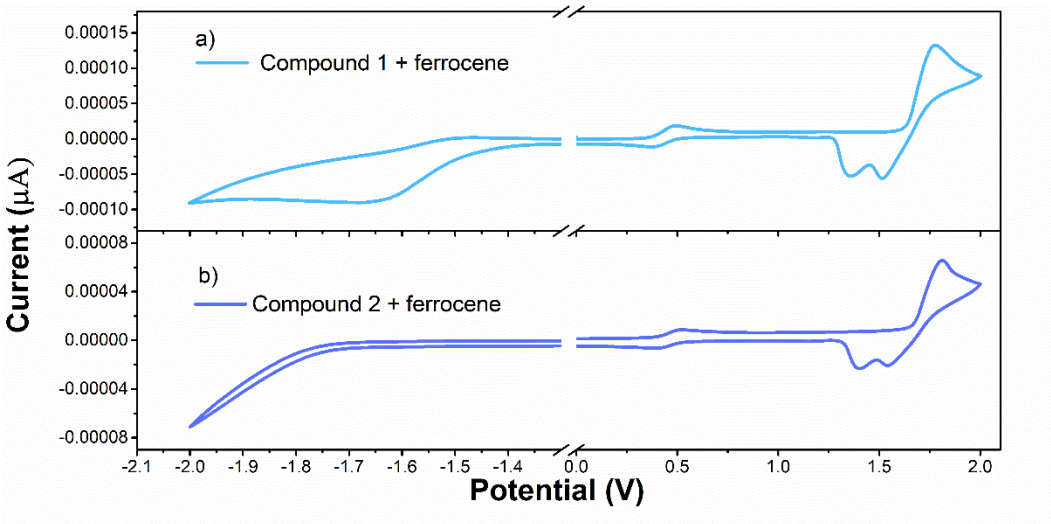

Fig. 30. CV curves of materials a) 1 and b) 2

3.3. UV enhanced emission

During photophysical experiments, it was observed that the emission of compound 1 changes if it gets exposed to UV light below 350 nm. Toluene solution of 1 emission intensified after it got treated by UV light. The intensity increased 13.6 times (figure 31 b). To check, if there is decomposition of material 1 because of UV light, the absorption spectra of toluene solution was measured before and after UV treatment (figure 31 a). There was no breaking in energy bands, new band appearance or similar effects.

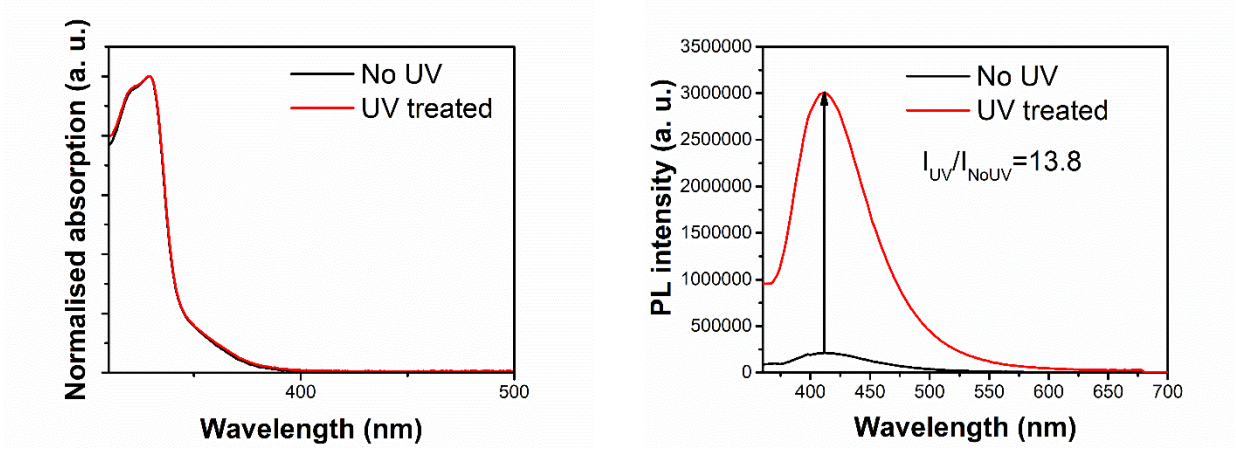

a) b)

Fig. 31. a) absorption spectra of non-treated and UV treated material 1 in THF solution, b) PL intensity of of non-treated and UV treated material 1 in toluene solution

The phenomena of enhanced emission occurred not only in toluene solution, but also in other, more polar solution, like THF or DMF. Not only intensity increased in these solutions, but the spectrum shifted to region of higher energy wavelengths. Intensity of compound 1 in THF increased 83.75 times and spectra maxima blue-shifted 39 nm, from 463 nm to 424 nm (figure 32 a). Similar situation with DMF solution. Intensity after 10 minutes of UV treatment increased 2.4 times and spectra blue-shifted 88 nm (figure 32 b).

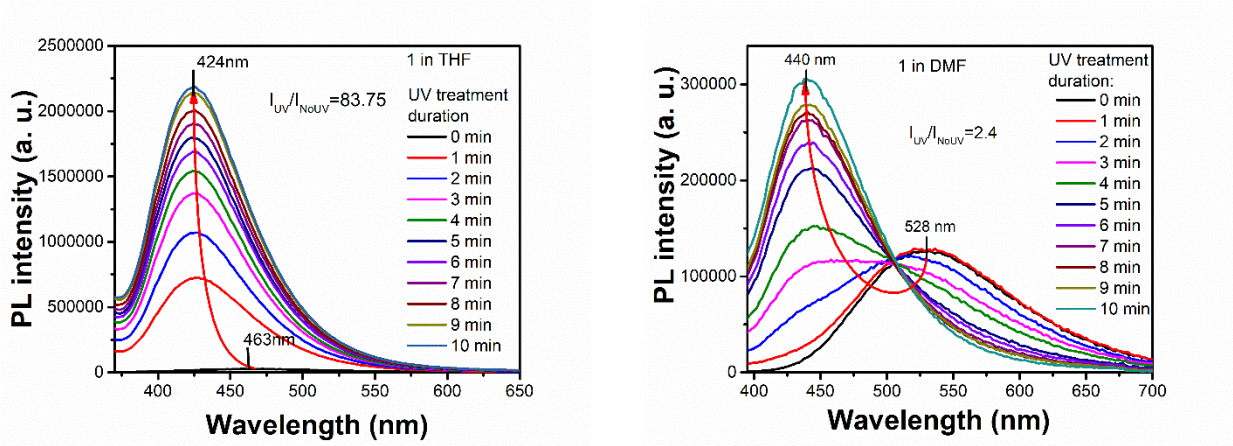

a) b)

Fig. 32. PL dependence on UV treatment time of material 1 a) THF solvent, b) DMF solvent

After UV treatment, blue-shifted maxima still depend on the polarity of the solvent. What this means that even if the solvent is UV treated, there is still solvatochromic effect. Which means that there is still CT state formation. As showed in figure 27 a, Lippert–Matagga plot, there is dependence between

Stokes shift and orientation polarizability. The slope of treated solvents is much smaller than non-treated, 5105 cm^{-1}, which can be explained by weaker CT formation.

The PL intensity of toluene solution increases, as the temperature increases, as showed in figure 33. This can be explained by ISC and RISC processes, which effectiveness increases as temperature increases. CT state formation, solvatochromic effect, triplet harvest and intensity increasement as the temperature increases leads to conclusion, that material 1 has TADF properties.

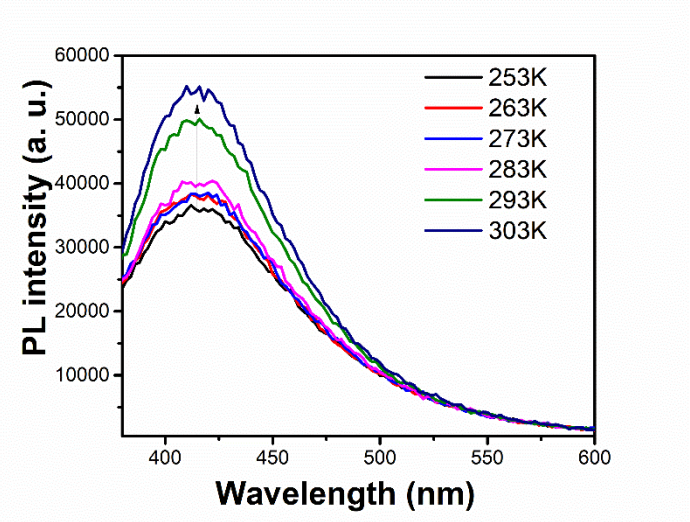

Fig. 33. UV **treated** material 1 in toluene solution PL dependence on temperature

The UV caused PL intensity enhancement can be explained by changes in molecular conformation. Two crystals were grown from acetone solution, one part of the solution was UV treated. As it can be seen from X-ray images of molecular structure, the conformation of not treated and treated crystals are different. The middle part, benzophenone moiety, without treatment is plane, but after UV treatment, this part gets twisted. This twisting, caused by UV light, may be the reason of the induced emission and spectra shifts.

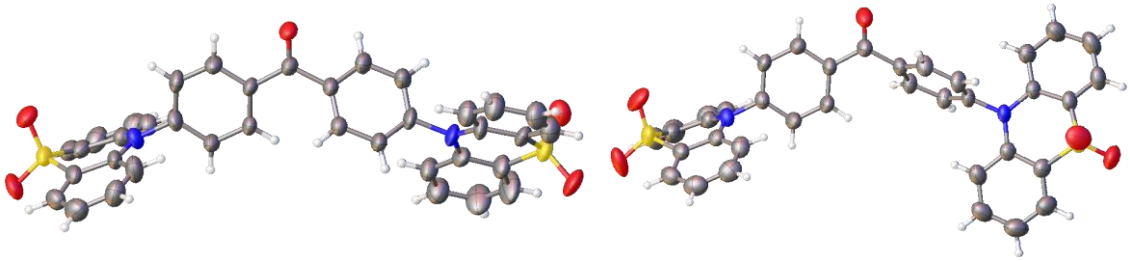

a) b)

Fig. 34. Crystal structure of crystals of material 1 grown from solution that was a) non treated b) UV treated

3.4. OLED devices

Material 1 and 2 were used as an emitter in OLED devices, A1 and A2 respectively. The structure of A1 and A2 is given in figure 24. Surrounding layers were chosen by their appropriate *HOMO – LUMO* levels. These were non-doped simple structure devices.

Device A1 showed non-uniformed EL spectra. A shoulder was noticed in the range 345–400 nm. This shoulder appeared because of recombination in mCP layer. As the applied voltage increased the

spectra maxima shifted to the lower energy wavelength region (table 4, figure 35a). The turn-on voltage was 6.8 V. The maximum brightness reached 1130 cd/m^2, which is decent brightness for computer displays and portable electronic devices (figure 12). The *CE* and *PE* reached 4.1 cd/A and 2.1 lm/W, respectively. The *EQE* reached 1.2% (table 4, figure 35b).

Table 4. Manufactured OLEDs characteristics

Device	EML	λ, nm	Turn-on voltage V_{ON}, V	Luminescence max, cd/m^2	CE_{MAX}, cd/A	PE_{MAX}, lm/W	EQE_{MAX}, %
A1	1	495/521/539	6.8	1130	2.8	1.4	1.2
A2	2	473	7.2	1060	1.1	0.49	0.52

A2 device performance was not great either. The turn-on voltage was 7.2 V and the maximum brightness was 1060 cd/m^2. This brightness, as the in A1 device, for portable electronic displays. The EL spectra were more uniform than A1 device. As the voltage increases EL spectrum becomes narrower. The spectra maxima were 473 nm (table 4, figure 35c). Maximum *CE*, *PE* and *EQE* values reached 1.1 cd/A, 0.5 lm/W and 0.5%, respectively (figure 35d). The efficiencies could increase for both devices, if device structure would be optimized.

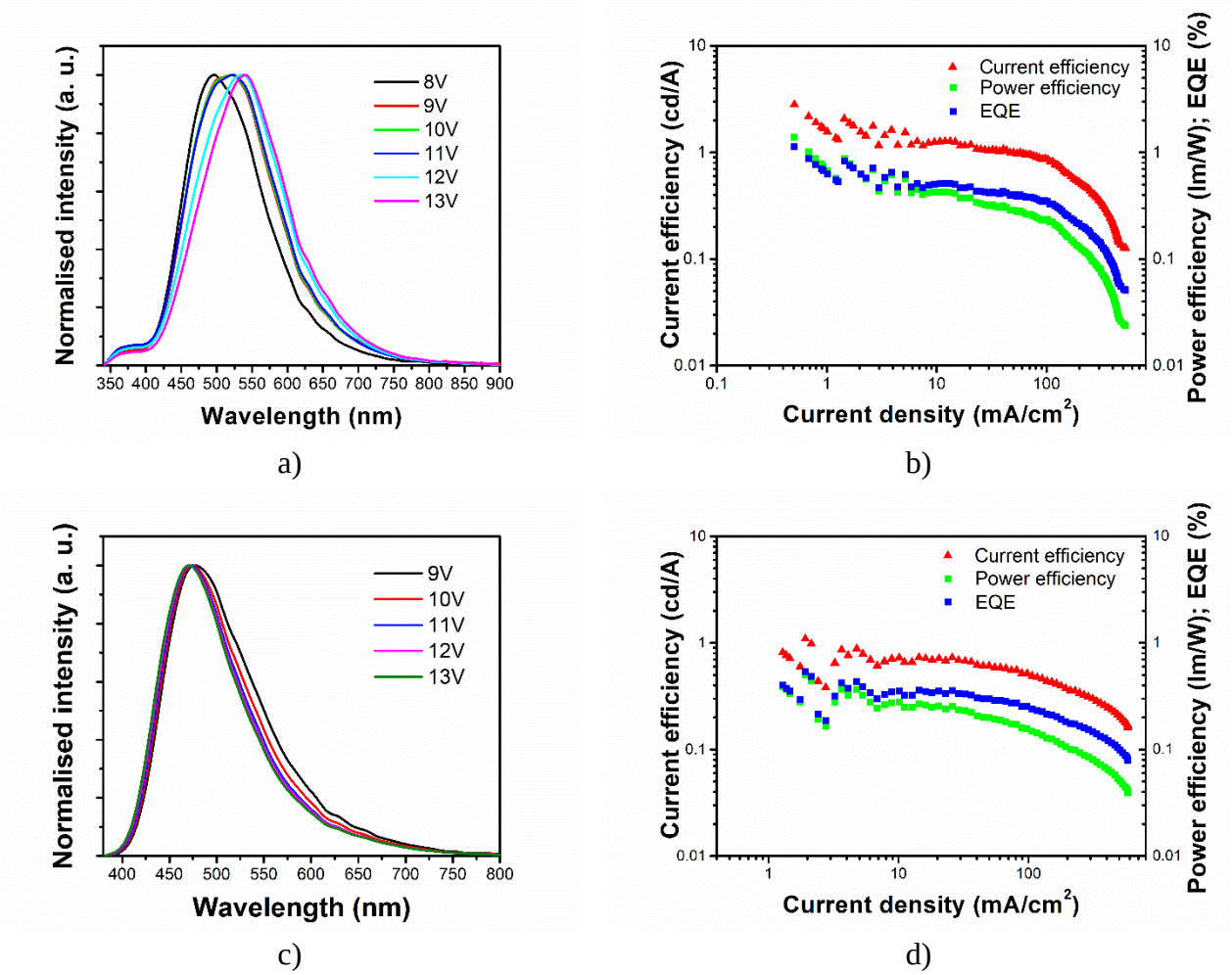

Fig. 35. EL spectra of OLED devices a) A1, c) A2 and current, power and external quantum efficiencies of devices b) A1, d) A2

3.5. Ultraviolet radiation dosimeter.

After establishing that UV induced conformational changes that leads to PL enhancement exist in material 1, it was decided, that solutions with compound 1 should be used as optical sensor. In this study three different solutions, toluene, THF and DMF, were used, to see how solvent affects material sensitivity and how the emission changes due to power of the UV light. First was measured toluene solution (figure 36). As the power increased the PL intensity also increases. For comparison, the PL intensity increases almost 2.4 times as the UV source power got increased from 0 µW to 145 µW. As showed in figure 35b, there is linear dependency between PL spectra area and power of UV treatment (slope was 35800 (R^2 = 0.99)).

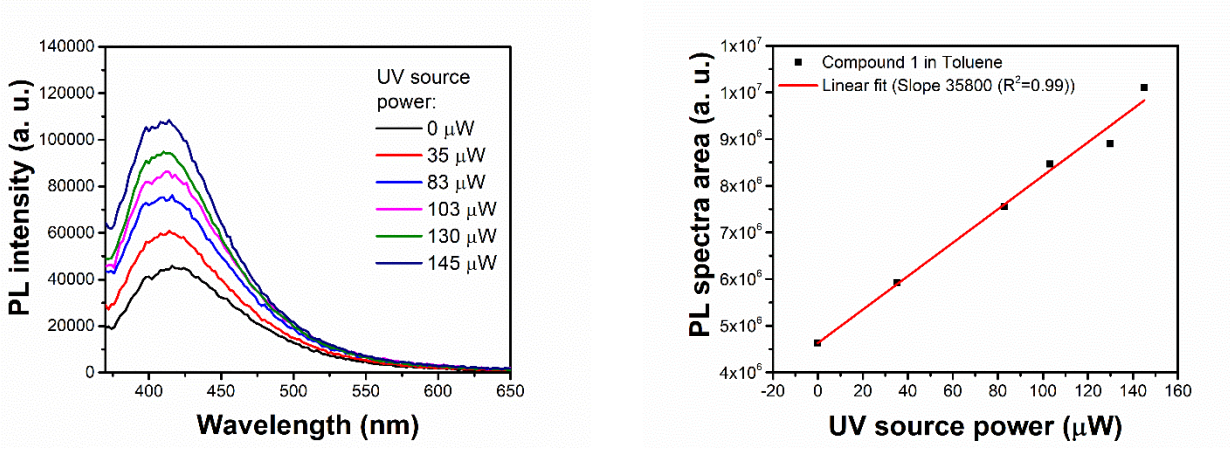

a) b)

Fig. 36. a) PL spectra of 1 in toluene solution at UV treatment powers b) PL intensity dependence on UV source used for treatment

The THF solution showed different results. As showed in figure 37a, the PL intensity increased drastically as the UV source power increased. As it is showed in figure 37b, the PL area considerably increased when UV source power was more than 100 µW. Also, it needs to be noted, that the rapid increasement stops after 200 µW, because solvent got saturated and no more conformational changes happen. It could be said, that the THF solution of compound 1 is most sensitive, when the UV source power is between 100 µW and 200 µW, where the slope of linear fit is 81000 (R^2 = 0.95)

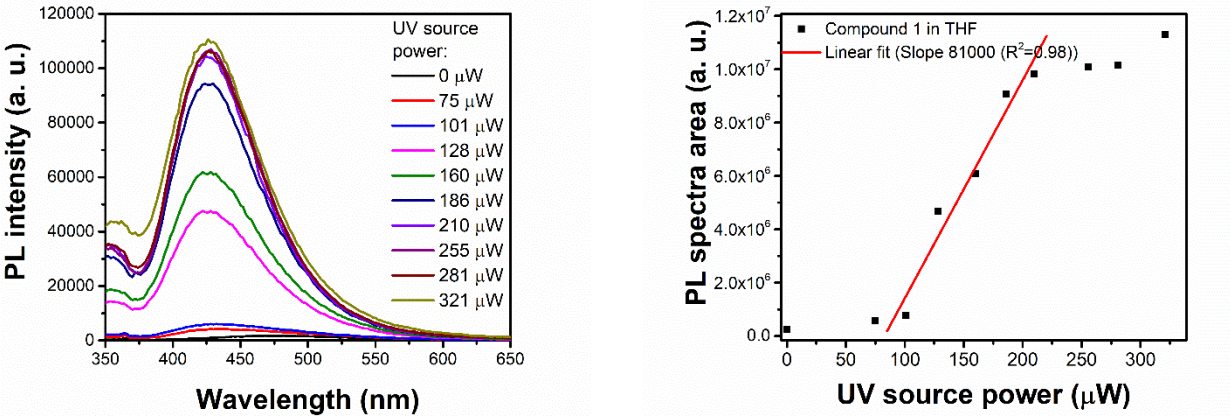

a) b)

Fig. 37. a) PL spectra of 1 in THF solution at UV treatment powers b) PL area dependence on UV source used for treatment power

Sensitivity measurements of DMF solution showed, that material in this solvent is not as sensitive as in THF. In the beginning the intensity of the spectra increased. As it showed in figure 38 b, increasement of PL spectra plot slows down in the 87–187 μW range. In this range intensity did not increased but the spectra shifted to higher energy wavelength region. After the shift intensity started to increase again. Sensing properties in this solvent are quite interesting, because there is almost a linear dependence between emission colour and UV source power (in the range of CIE coordinates from (0.29; 0.45) to (0.17; 0.16)) (figure 38 c). All in all, compound 1 in DMF solution showed the best sensitivity properties, because linear fit of spectra area dependence on UV power (figure 38 b) had the highest slope value, 115500 (R^2 = 0.93).

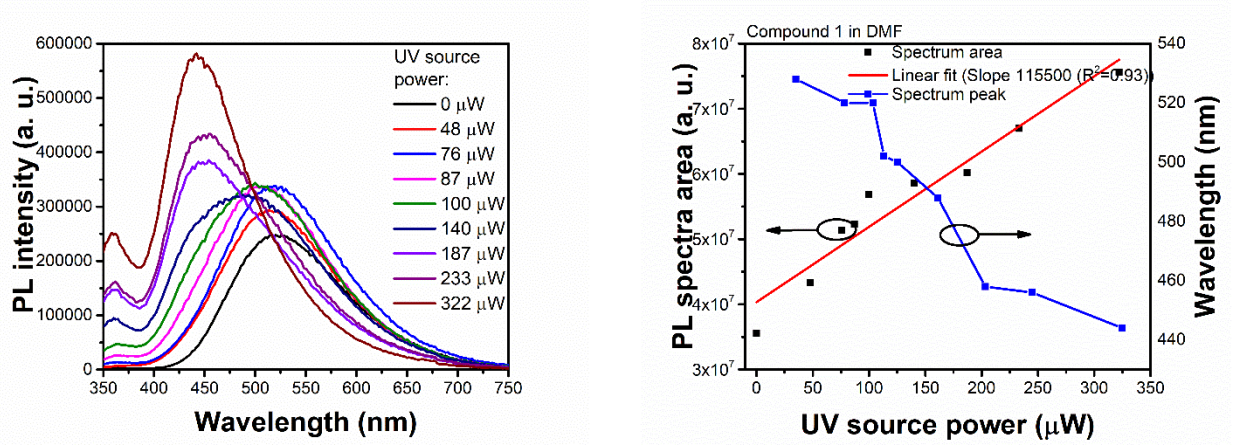

a) b)

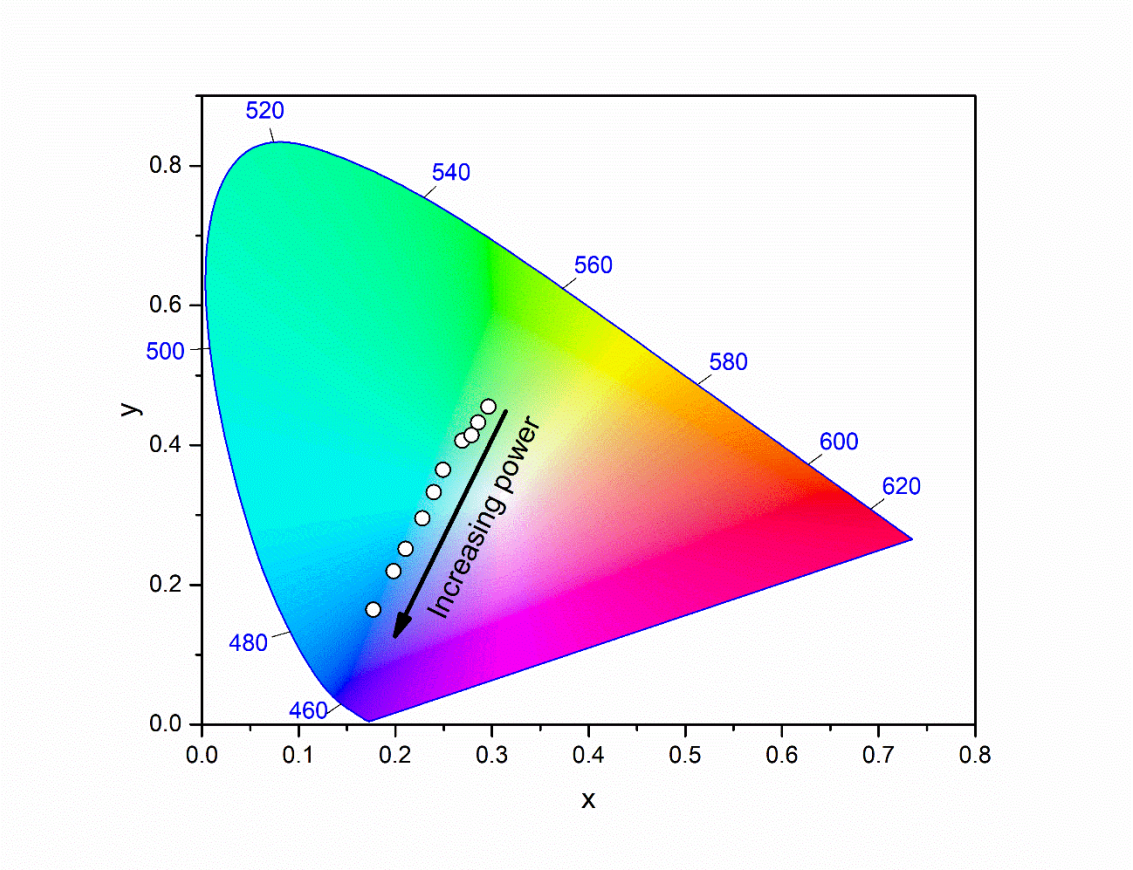

c)

Fig. 38. a) PL spectra of 1 in DMF solution at UV treatment powers b) PL area dependence on UV source power, c) CIE 1931 coordinates dependence on UV source used for treatment power

Conclusions

1. According to the photophysical investigations, benzophenone and sulfonyldi-phenylene derivatives were characterized by deep blue emission with PL spectra peaked at 416 nm and 397 nm in toluene solution, respectively. Photoluminescence quantum yield values of 7.4% and 9.3% were recorded for the benzophenone and sulfonyldi-phenylene derivative in solid state films, respectively. Both materials showed positive solvatochromic effect which related to charge transfer behaviour of their emission. The derivative of benzophenone showed the highest slope value of 19860 cm^{-1} in Lippert–Matagga plot demonstrating its higher dipole moment in comparison to that of the preference compound (sulfonyldi-phenylene derivative).
2. Both materials in toluene solution showed photoluminescence intensity increase after oxygen removal. Acetonitrile solutions of benzophenone and sulfonyldi-phenylene derivatives showed longer emission decay times after oxygen removal. This allowed to characterise these materials as thermally activated delayed fluorescence emitters.
3. In contrast to that of sulfonyldi-phenylene derivative, UV treatment of benzophenone derivative in different solutions led to either its enhanced photoluminescence intensity or colour changes. The emission intensity was increased and spectra was shifted to the higher energy wavelengths in comparison to the non-treated solutions. The enhancement is explained by conformational changes in molecular structure of benzophenone derivative which occurred under UV excitation.
4. Electroluminescent properties of benzophenone and sulfonyldi-phenylene derivatives as emitters were investigated in simply structured non-doped devices. The best device based on benzophenone derivative showed sky-blue electroluminescence and *EQE* values reaching 1.2%. Device based on sulfonyldi-phenylene derivative showed also sky-blue EL and *EQE* of 0.5%. Such results are in good agreement with *PLQY* of benzophenone and sulfonyldi-phenylene derivatives in solid-state.
5. The caused by UV photoluminescence enhancement light ability of benzophenone derivative allowed to use it as sensor material for detection of UV light intensity. Toluene, THF and DMF solutions, that benzophenone derivative was in, showed different sensitivity. THF solution showed stronger susceptibility to UV light (its intensity enhancements up to 83 times), while DMF solution showed wider visual emission changes (in the range of CIE coordinates from (0.29; 0.45) to (0.17; 0.16)) under UV excitation of different power and it was the most sensitive to UV light (Slope 115500 (R^2 = 0.93)).

List of references

1. Organic and Inorganic Photonics and Electronics | Materials | Georgia Institute of Technology | Atlanta, GA. [online]. [Accessed 25 April 2020 a]. Available from: http://www.materials.gatech.edu/core-strengths/organic-and-inorganic-photonics-and-electronics
2. OLED Info | The OLED Experts. [online]. [Accessed 15 May 2019 b]. Available from: https://www.oled-info.com/
3. JEN, Alex K.Y., 2010c. *Editorial: Interface engineering of organic electronics*. 16 March 2010. Royal Society of Chemistry.
4. BAEG, Kang Jun, BINDA, Maddalena, NATALI, Dario, CAIRONI, Mario and NOH, Yong Young, 2013d. *Organic light detectors: Photodiodes and phototransistors*. 21 August 2013.
5. KROTKUS, Simonas, 2016e. Advances in Organic Displays and Lighting. [online]. 2016. Available from: https://tud.qucosa.de/landing-page/?tx_dlf[id]=https%3A%2F%2Ftud.qucosa.de%2Fapi%2Fqucosa%253A30995%2Fmets
6. TANG, C. W. and VANSLYKE, S. A., 1987f. Organic electroluminescent diodes. *Applied Physics Letters* [online]. 21 September 1987. Vol. 51, no. 12, p. 913–915. [Accessed 5 April 2020]. DOI 10.1063/1.98799. Available from: http://aip.scitation.org/doi/10.1063/1.98799
7. MÉHES, Gábor, GOUSHI, Kenichi, POTSCAVAGE, William J. and ADACHI, Chihaya, 2014g. Influence of host matrix on thermally-activated delayed fluorescence: Effects on emission lifetime, photoluminescence quantum yield, and device performance. *Organic Electronics* [online]. 1 September 2014. Vol. 15, no. 9, p. 2027–2037. [Accessed 10 December 2018]. DOI 10.1016/j.orgel.2014.05.027. Available from: https://linkinghub.elsevier.com/retrieve/pii/S1566119914002067
8. SEREVIČIUS, Tomas, BUČIŪNAS, Tadas, BUCEVIČIUS, Jonas, DODONOVA, Jelena, TUMKEVIČIUS, Sigitas, KAZLAUSKAS, Karolis and JURŠĖNAS, Saulius, 2018h. Room temperature phosphorescence *vs.* thermally activated delayed fluorescence in carbazole–pyrimidine cored compounds. *Journal of Materials Chemistry C*. October 2018. Vol. 6, no. 41, p. 11128–11136. DOI 10.1039/C8TC02554A.
9. TANAKA, Hiroyuki, SHIZU, Katsuyuki, MIYAZAKI, Hiroshi and ADACHI, Chihaya, 2012i. Efficient green thermally activated delayed fluorescence (TADF) from a phenoxazine–triphenyltriazine (PXZ–TRZ) derivative. *Chemical Communications* [online]. 29 October 2012. Vol. 48, no. 93, p. 11392. [Accessed 15 May 2019]. DOI 10.1039/c2cc36237f. Available from: http://xlink.rsc.org/?DOI=c2cc36237f
10. ZHANG, Qisheng, LI, Jie, SHIZU, Katsuyuki, HUANG, Shuping, HIRATA, Shuzo, MIYAZAKI, Hiroshi and ADACHI, Chihaya, 2012j. Design of Efficient Thermally Activated Delayed Fluorescence Materials for Pure Blue Organic Light Emitting Diodes. *Journal of the American Chemical Society* [online]. 12 September 2012. Vol. 134, no. 36, p. 14706–14709. [Accessed 10 December 2018]. DOI 10.1021/ja306538w. Available from: http://www.ncbi.nlm.nih.gov/pubmed/22931361
11. LIAO, Caizhi, ZHANG, Meng, YAO, Mei Yu, HUA, Tao, LI, Li and YAN, Feng, 2015k. *Flexible Organic Electronics in Biology: Materials and Devices*. 2015. Wiley-VCH Verlag.
12. RIM, You Seung, BAE, Sang Hoon, CHEN, Huajun, DE MARCO, Nicholas and YANG, Yang, 2016l. *Recent Progress in Materials and Devices toward Printable and Flexible*

Sensors. 8 June 2016. Wiley-VCH Verlag.
13. WANG, Naixiang, YANG, Anneng, FU, Ying, LI, Yuanzhe and YAN, Feng, 2019m. Functionalized Organic Thin Film Transistors for Biosensing. *Accounts of Chemical Research*. 2019. DOI 10.1021/acs.accounts.8b00448.
14. OHRING, Milton, 1995n. ELECTRICAL PROPERTIES OF METALS, INSULATORS, AND DIELECTRICS. In: *Engineering Materials Science*. Academic Press. p. 559–610. ISBN 978-0-12-524995-9.
15. ASHCROFT, Neil W. and MERMIN, David, 1976o. *Solid State Physics*. Holt, Rinehart and Winston. ISBN 9780030839931.
16. RABE, Karin M., 2002p. Band Theory and Electronic Properties of SolidsBand Theory and Electronic Properties of Solids , John Singleton Oxford U. Press, New York, 2001. $70.00, $35.00 paper (222 pp.). ISBN 0-19-850645-7, ISBN 0-19-850644-9 paper . *Physics Today*. December 2002. Vol. 55, no. 12, p. 61–62. DOI 10.1063/1.1537918.
17. YU, Peter Y and CARDONA, Manuel, 1997q. Fundamentals of Semiconductors Physics and Materials Properties. [online]. 1997. [Accessed 30 March 2020]. DOI 10.1007/b137661. Available from: https://www.researchgate.net/publication/234337737
18. KITTEL, Charles., 2005r. *Introduction to solid state physics*. Wiley. ISBN 0471680575.
19. BRÜTTING, Wolfgang and ADACHI, Chihaya, 2013s. *Physics of Organic Semiconductors: Second Edition*. ISBN 9783527410538.
20. BRÉDAS, J. L., CALBERT, J. P., DA SILVA FILHO, D. A. and CORNIL, J., 2002t. Organic semiconductors: A theoretical characterization of the basic parameters governing charge transport. *Proceedings of the National Academy of Sciences of the United States of America*. 30 April 2002. Vol. 99, no. 9, p. 5804–5809. DOI 10.1073/pnas.092143399.
21. DEY, Anamika, SINGH, Ashish, DAS, Dipjyoti and IYER, Parameswar Krishnan, 2015u. Organic semiconductors: A new future of nanodevices and applications. In: *Thin Film Structures in Energy Applications*. Springer International Publishing. p. 97–128. ISBN 9783319147741.
22. FUKUI, Kenichi, 1975v. Singlet-Triplet Selectivity. In: . Springer, Berlin, Heidelberg. p. 81–83.
23. OILI PEKKOLA, 2017w. Investigations on the stability of poly(phenylene vinylene)-based organic light-emitting diodes. In: . Darmstadt. 2017. p. 115.
24. GALSIN, Joginder Singh, [no date]. *Solid state physics : an introduction to theory*. ISBN 9780128171042.
25. LA ROCCA, G.C, 2003y. Wannier–Mott Excitons in Semiconductors. In: . Academic Press. p. 97–128.
26. KÖHLER, Anna and BÄSSLER, Heinz, 2015z. Electronic and Optical Processes of Organic Semiconductors. In: *Electronic Processes in Organic Semiconductors* [online]. Weinheim, Germany: Wiley-VCH Verlag GmbH & Co. KGaA. p. 193–305. [Accessed 8 April 2020]. Available from: http://doi.wiley.com/10.1002/9783527685172.ch3
27. LICHTMAN, Jeff W. and CONCHELLO, José Angel, 2005aa. *Fluorescence microscopy*. December 2005.
28. KNIGHT, P.L., 1987ab. *Photons and Continuum States of Atoms and Molecules* [online]. Berlin, Heidelberg: Springer Berlin Heidelberg. [Accessed 8 April 2020]. Springer Proceedings in Physics. ISBN 978-3-642-71780-2. Available from: http://link.springer.com/10.1007/978-3-642-71778-9

29. OMARY, Mohammad A. and PATTERSON, Howard H., 1999ac. Luminescence Theory. In: *Encyclopedia of Spectroscopy and Spectrometry*. Elsevier. p. 1186–1207.
30. RURACK, Knut, 2008ad. Fluorescence Quantum Yields: Methods of Determination and Standards. In: *Standardization and Quality Assurance in Fluorescence Measurements I*. Springer Berlin Heidelberg. p. 101–145.
31. JAMESON, DAVID M., 2019ae. *INTRODUCTION TO FLUORESCENCE*. CRC PRESS. ISBN 9780367865702.
32. FERNÁNDEZ-ARGÜELLES, María Teresa, ENCINAR, Jorge Ruiz, SANZ-MEDEL, Alfredo and COSTA-FERNÁNDEZ, José M., 2019af. Phosphorescence | principles and instrumentation. In: *Encyclopedia of Analytical Science*. Elsevier. p. 284–291. ISBN 9780081019832.
33. SCHROGEL, Pamela, 2011ag. Novel Host Materials for Blue Phosphorescent Organic Light-Emitting Diodes. *Faculty of Biology, Chemistry and Earth Sciences*. 2011. Vol. Doctor of.
34. DELORME, R. and PERRIN, F., 1929ah. Durées de fluorescence des sels d'uranyle solides et de leurs solutions,. *Journal de Physique et le Radium* [online]. 1929. Vol. 10, no. 5, p. 177–186. [Accessed 3 April 2020]. DOI 10.1051/jphysrad:01929001005017700. Available from: http://www.edpsciences.org/10.1051/jphysrad:01929001005017700
35. BEZVIKONNYI, Oleksandr, GUDEIKA, Dalius, VOLYNIUK, Dmytro, MIMAITE, Viktorija, SEBASTINE, Bernard Ronit and GRAZULEVICIUS, Juozas V., 2019ai. Effect of donor substituents on thermally activated delayed fluorescence of diphenylsulfone derivatives. *Journal of Luminescence* [online]. 1 February 2019. Vol. 206, p. 250–259. [Accessed 7 March 2019]. DOI 10.1016/J.JLUMIN.2018.10.018. Available from: https://www.sciencedirect.com/science/article/pii/S0022231318310676
36. DIAS, Fernando B., BOURDAKOS, Konstantinos N., JANKUS, Vygintas, MOSS, Kathryn C., KAMTEKAR, Kiran T., BHALLA, Vandana, SANTOS, José, BRYCE, Martin R. and MONKMAN, Andrew P., 2013aj. Triplet harvesting with 100% efficiency by way of thermally activated delayed fluorescence in charge transfer OLED emitters. *Advanced Materials*. 19 July 2013. Vol. 25, no. 27, p. 3707–3714. DOI 10.1002/adma.201300753.
37. ANDREWS, David L. and BRADSHAW, David S., 2018ak. *Introduction to photon science and technology*. ISBN 9781510621954.
38. MEDINTZ, Igor and HILDEBRANDT, Niko, 2013al. *FRET - Förster Resonance Energy Transfer: From Theory to Applications* [online]. Wiley-VCH Verlag. [Accessed 8 April 2020]. ISBN 9783527656028. Available from: https://onlinelibrary.wiley.com/doi/book/10.1002/9783527656028
39. REINEKE, Sebastian, LINDNER, Frank, SCHWARTZ, Gregor, SEIDLER, Nico, WALZER, Karsten, LÜSSEM, Björn and LEO, Karl, 2009am. White organic light-emitting diodes with fluorescent tube efficiency. *Nature*. 14 May 2009. Vol. 459, no. 7244, p. 234–238. DOI 10.1038/nature08003.
40. LENK (GEB. HOFMANN), Simone, 2012an. Exciton Dynamics in White Organic Light-Emitting Diodes comprising Triplet Harvesting. *Qucosa.De* [online]. 2012. Available from: http://nbn-resolving.de/urn:nbn:de:bsz:14-qucosa-117447
41. SASAKI, Shunsuke, DRUMMEN, Gregor P.C. and KONISHI, Gen Ichi, 2016ao. Recent advances in twisted intramolecular charge transfer (TICT) fluorescence and related phenomena in materials chemistry. *Journal of Materials Chemistry C* [online]. 2016. Vol. 4, no. 14, p. 2731–2743. DOI 10.1039/c5tc03933a. Available from:

http://dx.doi.org/10.1039/C5TC03933A
42. DAINTITH, John, 2008ap. A Dictionary of chemistry. *Choice Reviews Online*. 2008. Vol. 46, no. 04, p. 46-1825-46–1825. DOI 10.5860/choice.46-1825.
43. GEFFROY, Bernard, LE ROY, Philippe and PRAT, Christophe, 2006aq. Organic light-emitting diode (OLED) technology: Materials, devices and display technologies. *Polymer International*. 2006. Vol. 55, no. 6, p. 572–582. DOI 10.1002/pi.1974.
44. SYCH, Galyna, SIMOKAITIENE, Jurate, BEZVIKONNYI, Oleksandr, TSIKO, Uliana, VOLYNIUK, Dmytro, GUDEIKA, Dalius and GRAZULEVICIUS, Juozas V, 2018ar. Exciplex-Enhanced Singlet Emission Efficiency of Nondoped Organic Light Emitting Diodes Based on Derivatives of Tetrafluorophenylcarbazole and Tri/Tetraphenylethylene Exhibiting Aggregation-Induced Emission Enhancement. *J. Phys. Chem. C* [online]. 2018. Vol. 122, p. 13. [Accessed 2 December 2018]. DOI 10.1021/acs.jpcc.8b03895. Available from: https://pubs.acs.org/sharingguidelines
45. BIRMINGHAM, J. M. and WILKINSON, G., 1956as. The Cyclopentadienides of Scandium, Yttrium and Some rare Earth Elements. *Journal of the American Chemical Society* [online]. 1 January 1956. Vol. 78, no. 1, p. 42–44. [Accessed 5 April 2020]. DOI 10.1021/ja01582a009. Available from: https://pubs.acs.org/doi/abs/10.1021/ja01582a009
46. KUMATANI, Akichika, LI, Yun, DARMAWAN, Peter, MINARI, Takeo and TSUKAGOSHI, Kazuhito, 2013at. On practical charge injection at the metal/organic semiconductor interface. *Scientific Reports*. 4 January 2013. Vol. 3, no. 1, p. 1–6. DOI 10.1038/srep01026.
47. LE CORRE, Vincent M., STOLTERFOHT, Martin, PERDIGÓN TORO, Lorena, FEUERSTEIN, Markus, WOLFF, Christian, GIL-ESCRIG, Lidón, BOLINK, Henk J., NEHER, Dieter and KOSTER, L. Jan Anton, 2019au. Charge Transport Layers Limiting the Efficiency of Perovskite Solar Cells: How to Optimize Conductivity, Doping, and Thickness. *ACS Applied Energy Materials*. 23 September 2019. Vol. 2, no. 9, p. 6280–6287. DOI 10.1021/acsaem.9b00856.
48. NEGI, Shubham, MITTAL, Poornima and KUMAR, Brijesh, 2018av. Impact of different layers on performance of OLED. *Microsystem Technologies*. 1 December 2018. Vol. 24, no. 12, p. 4981–4989. DOI 10.1007/s00542-018-3918-y.
49. YERSIN, H. (Hartmut) and WILEY INTERSCIENCE (ONLINE SERVICE), 2007aw. *Highly efficient OLEDs with phosphorescent materials* [online]. Wiley-VCH. [Accessed 10 December 2018]. ISBN 9783527405947. Available from: https://www.wiley.com/en-us/Highly+Efficient+OLEDs+with+Phosphorescent+Materials-p-9783527405947
50. DE, Daniel, PEREIRA, Sá, DATA, Przemyslaw and MONKMAN, Andrew P, [no date]. *Methods of Analysis of Organic Light Emitting Diodes †*.
51. REINEKE, Sebastian, 2009ay. Controlling Excitons : Concepts for Phosphorescent Organic LEDs at High Brightness Sebastian Reineke. *Arbeit* [online]. 2009. No. November. Available from: https://tud.qucosa.de/landing-page/?tx_dlf[id]=https%3A%2F%2Ftud.qucosa.de%2Fapi%2Fqucosa%253A25358%2Fmets
52. SRIVASTAVA, Ritu, KAMALASANAN, M.N., CHAUHAN, Gayatri, KUMAR, Arunandan, TYAGI, Priyanka and KUMAR, Amit, 2010az. Organic Light Emitting Diodes

for White Light Emission. In: *Organic Light Emitting Diode*. Sciyo.

53. PENG, Jinghong, XU, Xinjun, FENG, Xin Jiang and LI, Lidong, 2018ba. Fabrication of solution-processed pure blue fluorescent OLED using exciplex host. *Journal of Luminescence* [online]. 1 June 2018. Vol. 198, p. 19–23. [Accessed 30 January 2019]. DOI 10.1016/j.jlumin.2018.02.010. Available from: https://www.sciencedirect.com/science/article/pii/S0022231317318355
54. DOS-SANTOS, PALOMA, LAYS, 2018bb. The Study of Thermally Activated Delayed Fluorescence Mechanism in Mono and Bimolecular Systems. *Thesis* [online]. 2018. Available from: http://etheses.dur.ac.uk/12840/
55. JOU, Jwo-Huei, KUMAR, Sudhir, AGRAWAL, Abhishek, LI, Tsung-Han and SAHOO, Snehashis, 2015bc. Approaches for fabricating high efficiency organic light emitting diodes. *Journal of Materials Chemistry C* [online]. 19 March 2015. Vol. 3, no. 13, p. 2974–3002. [Accessed 11 December 2017]. DOI 10.1039/C4TC02495H. Available from: http://xlink.rsc.org/?DOI=C4TC02495H
56. ALTAZIN, Stéphane, PENNINCK, Lieven and RUHSTALLER, Beat, 2018bd. Outcoupling Technologies: Concepts, Simulation, and Implementation. In: *Handbook of Organic Light-Emitting Diodes*. Springer Japan. p. 1–22.
57. MILLER, F P, VANDOME, A F and JOHN, M B, 2010be. *CIE 1931 Color Space* [online]. VDM Publishing. ISBN 9786130669973. Available from: https://books.google.lt/books?id=238tYAAACAAJ
58. FRADEN, Jacob, 2006bf. Sensor Characteristics. In: *Handbook of Modern Sensors*. New York: Springer-Verlag. p. 13–36. ISBN 978-0-387-21604-1.
59. GARCIA-BREIJO, Eduardo, PEREZ, Berta Gomez-Lor and COSSEDDU, Piero, 2016bg. *Organic Sensors: Materials and Applications*. Institution of Engineering and Technology. ISBN 184919985X.
60. TOMKEVICIENE, Ausra, DABULIENĖ, Asta, MATULAITIS, Tomas, GUZAUSKAS, Matas, ANDRULEVICIENE, Viktorija, GRAZULEVICIUS, Juozas Vidas, YAMANAKA, Yuri, YANO, Yoshio and ONO, Toshikazu, 2019bh. Bipolar thianthrene derivatives exhibiting room temperature phosphorescence for oxygen sensing. *Dyes and Pigments*. 1 November 2019. Vol. 170. DOI 10.1016/j.dyepig.2019.107605.
61. BAIERL, Daniela, PANCHERI, Lucio, SCHMIDT, Morten, STOPPA, David, DALLA BETTA, Gian Franco, SCARPA, Giuseppe and LUGLI, Paolo, 2012bi. A hybrid CMOS-imager with a solution-processable polymer as photoactive layer. *Nature Communications* [online]. 2012. Vol. 3. [Accessed 8 April 2020]. DOI 10.1038/ncomms2180. Available from: www.nature.com/naturecommunications
62. LIN, Hui, YU, Jun sheng and ZHANG, Wei, 2012bj. Investigation of top-emitting OLEDs using molybdenum oxide as anode buffer layer. *Optoelectronics Letters*. May 2012. Vol. 8, no. 3, p. 197–200. DOI 10.1007/s11801-012-1189-x.
63. [5,6]-Fullerene-C70 98% | Fullerene-C70 | Sigma-Aldrich, [no date]. [online]. [Accessed 10 April 2020 bk]. Available from: https://www.sigmaaldrich.com/catalog/product/aldrich/482994?lang=en&region=LT
64. CHAPRAN, Marian, LYTVYN, Roman, BEGEL, Corentin, WIOSNA-SALYGA, Gabriela, ULANSKI, Jacek, VASYLIEVA, Marharyta, VOLYNIUK, Dmytro, DATA, Przemyslaw and GRAZULEVICIUS, Juozas Vidas, 2019bl. High-triplet-level phthalimide based acceptors for exciplexes with multicolor emission. *Dyes and Pigments* [online]. 1 March 2019.

Vol. 162, p. 872–882. [Accessed 7 March 2019]. DOI 10.1016/J.DYEPIG.2018.11.022. Available from: https://www.sciencedirect.com/science/article/pii/S0143720818321788

65. TSPO1 | Sigma-Aldrich, [no date]. [online]. [Accessed 10 April 2020 bm]. Available from: https://www.sigmaaldrich.com/catalog/product/aldrich/901444?lang=en&region=LT&gclid=CjwKCAjwssD0BRBIEiwA-JP5rJRI1POTWwvee8VnqS1dToIAX3V4UeZ79GXp5XaBKywSqp-FxGeO0hoCt0AQAvD_BwE
66. ZASSOWSKI, Pawel, LEDWON, Przemyslaw, KUROWSKA, Aleksandra, HERMAN, Artur P., LAPKOWSKI, Mieczyslaw, CHERPAK, Vladyslav, HOTRA, Zenon, TURYK, Pavlo, IVANIUK, Khrystyna, STAKHIRA, Pavlo, SYCH, Galyna, VOLYNIUK, Dmytro and GRAZULEVICIUS, Juozas Vidas, 2018bn. 1,3,5-Triazine and carbazole derivatives for OLED applications. *Dyes and Pigments* [online]. 2018. Vol. 149, no. July 2017, p. 804–811. DOI 10.1016/j.dyepig.2017.11.040. Available from: https://doi.org/10.1016/j.dyepig.2017.11.040
67. ZHANG, Chun-lin, WANG, Fang-cong, ZHANG, Yong, LI, Hai-xia and LIU, Su, 2010bo. Studying the Attribution of LiF in OLED by the - Characteristics. *International Journal of Photoenergy* [online]. 2 December 2010. Vol. 2010, p. 1–4. [Accessed 15 May 2019]. DOI 10.1155/2010/291931. Available from: http://www.hindawi.com/journals/ijp/2010/291931/
68. HUANG, Bin, QI, Qi, JIANG, Wei, TANG, Jinan, LIU, Yuanyuan, FAN, Wenjuan, YIN, Zhihui, SHI, Fachen, BAN, Xinxin, XU, Huange and SUN, Yueming, 2014bp. Thermally activated delayed fluorescence materials based on 3,6-di-tert-butyl-9-((phenylsulfonyl)phenyl)-9H-carbazoles. *Dyes and Pigments*. 1 December 2014. Vol. 111, p. 135–144. DOI 10.1016/j.dyepig.2014.06.008.

Students achievements

List of publications

1. **GUZAUSKAS, Matas**, VOLYNIUK, Dmytro, TOMKEVICIENE, Ausra, PIDLUZHNA, Anna, LAZAUSKAS, Algirdas and GRAZULEVICIUS, Juozas Vidas, 2019. Dual nature of exciplexes: exciplex-forming properties of carbazole and fluorene hybrid trimers. *Journal of Materials Chemistry C*. 2019. Vol. 7, no. 1, p. 25–32. DOI 10.1039/C8TC04708A.
2. TOMKEVICIENE, Ausra, MATULAITIS, Tomas, **GUZAUSKAS, Matas**, ANDRULEVICIENE, Viktorija, VOLYNIUK, Dmytro and GRAZULEVICIUS, Juozas Vidas, 2019. Thianthrene and acridan-substituted benzophenone or diphenylsulfone: Effect of triplet harvesting via TADF and phosphorescence on efficiency of all-organic OLEDS. *Organic Electronics*. 1 July 2019. Vol. 70, p. 227–239. DOI 10.1016/j.orgel.2019.04.025.
3. TOMKEVICIENE, Ausra, DABULIENĖ, Asta, MATULAITIS, Tomas, **GUZAUSKAS, Matas**, ANDRULEVICIENE, Viktorija, GRAZULEVICIUS, Juozas Vidas, YAMANAKA, Yuri, YANO, Yoshio and ONO, Toshikazu, 2019. Bipolar thianthrene derivatives exhibiting room temperature phosphorescence for oxygen sensing. *Dyes and Pigments*. 1 November 2019. Vol. 170. DOI 10.1016/j.dyepig.2019.107605.
4. KERUCKIENE, Rasa, **GUZAUSKAS, Matas**, NARBUTAITIS, Edgaras, TSIKO, Uliana, VOLYNIUK, Dmytro, LEE, Pei Hsi, CHEN, Chia Hsun, CHIU, Tien Lung, LIN, Chi Feng, LEE, Jiun Haw and GRAZULEVICIUS, Juozas Vidas, 2020. Exciplex-forming derivatives of 2,7-di-tert-butyl-9,9-dimethylacridan and benzotrifluoride for efficient OLEDs. *Organic Electronics*. 1 March 2020. Vol. 78, p. 105576. DOI 10.1016/j.orgel.2019.105576.
5. SYCH, Galyna, **GUZAUSKAS, Matas**, VOLYNIUK, Dmytro, SIMOKAITIENE, Jurate, STARYKOV, Hryhorii and GRAZULEVICIUS, Juozas V., 2020. Exciplex Energy Transfer through Spacer: White Electroluminescence with Enhanced Stability Based on Cyan Intermolecular and Orange Intramolecular Thermally Activated Delayed Fluorescence. *Journal of Advanced Research* [online]. 16 May 2020. [Accessed 18 May 2020]. DOI 10.1016/j.jare.2020.04.018. Available from: https://linkinghub.elsevier.com/retrieve/pii/S2090123220300801

Conferences

1. **GUŽAUSKAS, Matas**, VOLYNIUK, Dmytro, TOMKEVIČIENĖ, Aušra and GRAŽULEVIČIUS, Juozas Vidas, 2019. DEVELOPMENTS OF GREEN SOLUTION-PROCESSED ORGANIC LIGHT EMITTING DIODES EXPLOITING EXCIPLEX-FORMING HOSTS AND TADF EMITTERS. *Poster in "OpenReadings19" conferebce*. Vilnius. 2019. Available from: http://www.openreadings.eu/thesismanager/thesis19/P1-87.pdf
2. **GUZAUSKAS, Matas**, SNEIDERAITYTE, Aiste, VOLYNIUK, Dmytro, TOMKEVIČIENĖ, Aušra and GRAŽULEVIČIUS, Juozas Vidas, 2019. GREEN AYMMETRIC TADF MATERIALS FOR EFFICIENT OLED DEVICES. *Poster in "π-EJ 2019"*. Zabrze. 2019.
3. **GUZAUSKAS, Matas**, NARBUTAITIS, Edgaras, VOLYNIUK, Dmytro and GRAZULEVICIUS, Juozas Vidas, 2020. INVESTIGATION OF PHOTO INDUCED CONFORMATIONAL CHANGES IN ORGANIC FLUORESCENCE EMITTERS. *Poster in "OpenReading20"*. Vilnius. 2020. http://www.openreadings.eu/thesismanager/thesis20/821Guzauskas.pdf